



Natural acid rock drainage in alpine catchments: A side effect of climate warming

Mario Zarroca^{a,*}, Carles Roqué^b, Rogelio Linares^a, José G. Salmanci^{a,c}, Francisco Gutiérrez^d

^a Geology Department, Universitat Autònoma de Barcelona, E-08193-Bellaterra, Barcelona, Spain

^b Àrea de Geodinàmica Externa i Geomorfologia, Universitat de Girona, E-17071 Girona, Spain

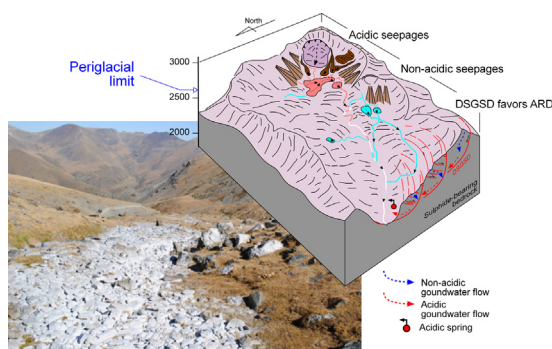
^c Geology and Environment Department, Instituto Nacional de Tecnología Industrial (INTI), Avenida General Paz 5445, Buenos Aires, Argentina

^d Earth Sciences Department, Universidad de Zaragoza, C/. Pedro Cerbuna 12, E-50009 Zaragoza, Spain

HIGHLIGHTS

- Historical mapping reveals strong intensification of high-mountain acidification.
- Natural acid rock drainages release potentially toxic metals into mountain habitats.
- Both climatic and geomorphological dynamics control the severity of the phenomenon.
- Natural acid rock drainages likely will intensify in a future due to climate warming.

GRAPHICAL ABSTRACT



ARTICLE INFO

Article history:

Received 23 December 2020

Received in revised form 13 February 2021

Accepted 20 February 2021

Available online 26 February 2021

Editor: Christian Herrera

Keywords:

Acidification

Alt Pirineu Natural Park (Central Pyrenees)

Climate change

High-mountain waters

Potentially toxic trace metals

ABSTRACT

A historical series of aerial photographs spanning more than 70 years (1945–2018) revealed that natural acid rock drainage (ARD) has experienced an intensification in the Noguera de Vallferrera alpine catchment (Central Pyrenees) due to climate change during the last decade. ARD manifests by the precipitation of whitish aluminum-compounds that strikingly cover the beds of some gullies and streams in high-mountain catchments. The total length of affected streams has increased from ca. 5 km (1945) to more than 35 km (2018). Up to 68 water samples were collected in three main areas to determine the spatial variation in acidity and concentration of dissolved metals, representative of surface and subsurface waters. Concentration of aluminum clearly correlates with acidity of waters. Aluminum precipitation occurs where acidic waters, enriched in metals due ARD related to the oxidation of sulfides, mix with non-acidic waters. In addition to aluminum, other potentially toxic trace metals are present at concentrations well above the quality standards for natural waters. Here, we show that climate warming and the severe droughts recorded in the last decade are the most plausible causes for the observed ARD intensification. This result is supported by a good correlation between the regional ascending rate of the periglacial limits (ca. 46 m-height/decade) and the rising rate of the maximum elevations at which ARD occurs (ca. 45 to 55 m-height/decade). In addition to climatic control, we also show that the local geomorphology is playing a major role. The distribution of periglacial deposits (rock glaciers, protalus ramparts, cones and talus slopes) and deep-seated gravitational slope deformations exert a strong control on the spatial patterns and hydrodynamics of ARD. A better understanding of the phenomenon and the monitoring of its evolution can provide clues on these side effects of climate warming, here and in many other alpine catchments worldwide.

© 2021 The Authors. Published by Elsevier B.V. This is an open access article under the CC BY-NC-ND license (<http://creativecommons.org/licenses/by-nc-nd/4.0/>).

* Corresponding author.

E-mail address: mario.zarroca.hernandez@uab.cat (M. Zarroca).

1. Introduction

Acid drainage is considered by the United Nations one of the most challenging environmental problems that society will face in the coming years (e.g. Tuffnell, 2017; Qian and Li, 2019). Acid drainage is the result of bio-chemical weathering of certain minerals contained in sulfide-bearing rocks under water and oxygen-rich environments (e.g. Nordstrom, 2011a). The interaction of sulfides as Pyrite (FeS_2) with oxygen and water results in the formation of sulfuric acid that attacks the rocks, dissolving Fe, Al and other minor elements (Nordstrom and Alpers, 1999; Bigham and Nordstrom, 2000; Blowes et al., 2004). Some of these elements, in non-elevated concentrations, are considered essential for life (e.g. Co, Cu, Zn, and Mn) (Mertz, 1981; Nielsen, 1990), whereas others (e.g. Cd, Hg, Pb, or As) either do not have any known physiological function and/or are very toxic, even at trace concentrations (Godt et al., 2006; Sarmiento et al., 2011; Olmedo et al., 2013). Therefore, acidic metal-enriched waters may cause severe degradation of water masses and damage to ecosystems (e.g. Nordstrom, 2009; Nordstrom, 2011a; Nordstrom, 2011b; Talukdar et al., 2016; Ilyashuk et al., 2018). In addition to solutes, metals also form precipitates. For example, Al, which is a major component of a number of common silicate minerals, generally precipitates at $\text{pH} > 4.5$ – 5.6 in the form of whitish-colored aluminum-hydroxides and -hydroxisulphates (AHPs) (Bigham and Nordstrom, 2000; Takeno, 2005; Sánchez-España et al., 2011, 2016; Gault et al., 2015).

Acid drainages are commonly linked to the mining industry (acid mine drainage, AMD) (Nordstrom, 2009). However, they may also occur in unmined catchments rich in sulfides under specific natural conditions (acid rock drainage, ARD) (Nordstrom and Alpers, 1999). Although the study of AMD has been extensively addressed in the literature (e.g. Plaza et al., 2017; Qian and Li, 2019; Rezaie and Anderson, 2020; Giddings et al., 2020; Galván et al., 2021), research dealing with the ARD phenomenon and the associated impacts is much more limited (e.g. Kwong et al., 2009; Todd et al., 2012; Ilyashuk et al., 2014, 2018;

Gault et al., 2015). The climate is alleged to exert a strong control on ARD processes (Furniss et al., 1999; Plumlee et al., 1999). Some observations made during the last decades suggest that climate change is promoting an increase in some water solutes in mountain areas with metal-sulfide mineralization (Manning et al., 2013), where ARD is the main natural mechanism for metal enrichment in waters. Studies conducted over 30 years in the southern sector of the Rocky Mountains (Colorado, USA) reveal that metals and SO_4^{2-} concentrations in water have increased up to 100–400% in recent years (e.g. Todd et al., 2012; Crouch et al., 2013; Manning et al., 2013). The warmer and drier conditions induced by the climate change are claimed to be the possible causes for the significant quality deterioration of rivers and groundwater in the region. This problem has been also documented in other mountain areas worldwide, such as the Yukon Territory (Canada) (Lacelle et al., 2007; Kwong et al., 2009; Gault et al., 2015); the Himalayas (Salerno et al., 2016); or the European Alps (Thies et al., 2007; Ilyashuk et al., 2014).

There is strong evidence supporting that the rate of warming is amplified by elevation (Pepin et al., 2015). The effects of elevation-dependent warming are especially significant in alpine environments. Warming rates have reached up to $+0.8$ °C/decade in the Tibetan Plateau since the last 50 yrs. (Pepin et al., 2015), and $+0.5$ °C/decade in the European Alps since the 1980s (EEA, 2009). In the Pyrenees (Fig. 1), the average temperature has raised ca. $+0.2$ to $+0.4$ °C/decade since the 1950s, which exceeds in 30% the world average (OPCC-CTP, 2018). Here, positive anomalies have been recorded systematically since 1980s, being the last decade the warmest since the start of the instrumental records (1910). This trend is even more pronounced in the central sector of the Pyrenees, where significant positive trends for temperature ($T = +0.23$ to 0.57 °C/decade) have been observed during the period 1970–2013, in contrast with the more subtle long-term (1910–2013) trends ($T = +0.11$ to $+0.06$ °C/decade) (Pérez-Zanón et al., 2017). General trends regarding precipitation are not as clear, since positive and negative anomalies alternate over short time spans

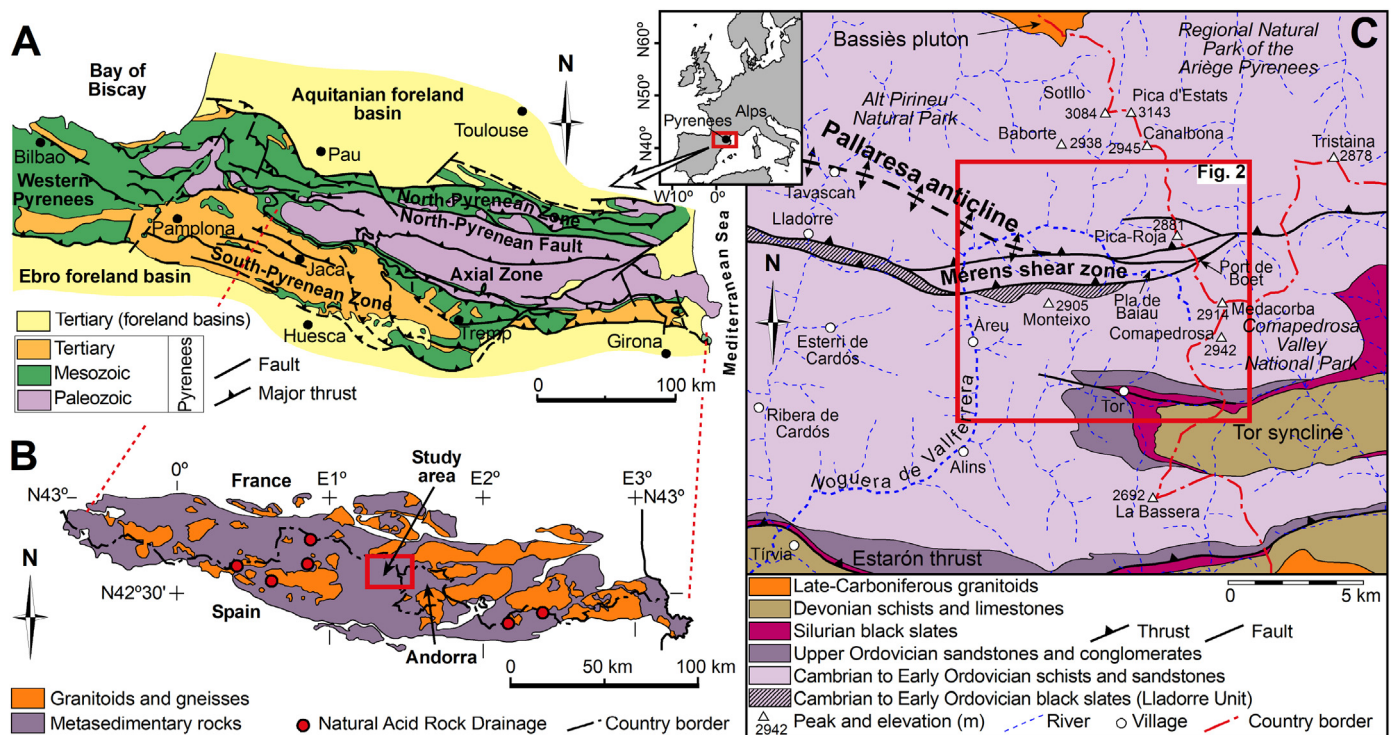


Fig. 1. Geological setting of the study area. (A) Geological sketch of the Pyrenees showing the main structural units (after Rosell and Linares, 2001). (B) Distribution of areas with evidence of natural acid rock drainage (ARD) in the Pyrenean axial zone, occurring in high-mountain catchments mainly underlain by sulphide-bearing metasedimentary rocks. (C) Simplified geological map of the eastern sector of the Alt Pirineu Natural Park. The Noguera de Vallfererra catchment (NVC) is associated with the Merens shear zone, where a thick succession of metasedimentary Silurian to early Ordovician formations crop out, including the pyrite-rich slates of the Lladorre Unit in the Monteixo-Norís Range.

for the same periods (OPCC-CTP, 2018). Precipitation negative trends have been reported for the eastern sector of the Pyrenees (-3 to -8% /decade), more pronounced since 1950 (BAIC, 2019). However, although this pattern is also observable in the central Pyrenees, the amplitude of the negative anomalies is rather small (-0.64% during 1910–1970; -2.70% for 1970–2013) (Pérez-Zanón et al., 2017; OPCC-CTP, 2018).

The Pyrenean region hosts the southernmost glaciers in Europe (Fig. 1A) and the warming has already caused a 50% reduction of the total glaciers reported in 1984 (OPCC-CTP, 2018). Periglacial rock deposits such as rock glaciers are climatically more resilient than glaciers to thaw (Jones et al., 2019), although they are also experiencing rapid degradation due to climate warming rapid degradation due to climate warming (e.g. Thies et al., 2007; Salerno et al., 2016; Ilyashuk et al., 2018). Rocky periglacial deposits may constitute high-permeability aquifers (Jones et al., 2019), and their thawing is reported to cause ARD in many cold mountains with sulfide mineralization (Williams et al., 2006; Todd et al., 2012; Ilyashuk et al., 2014). Climatic predictions do not foresee a change in the climate warming trend for the coming years (e.g. Radić et al., 2014; Huss and Hock, 2018), thus ARD could become more common and severe in many mountain regions worldwide. The consequences on the quality of water resources and ecosystems remain uncertain.

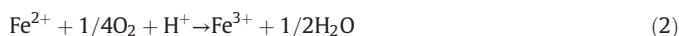
Here we aim at investigating the ARD processes occurring in the Noguera of Vallferrera catchment (NVC) (Alt Pirineu Natural Park, Central Pyrenees) (Fig. 1). In this regard, this research attempts to provide a scientific basis on ARD that could be useful for designing effective adaptation strategies to the impacts of climate warming on water resources and ecological value of mountain habitats. The main specific objectives of the research are (1) to identify the scope of the ARD processes in the NVC, (2) to study their evolution during the last decades; and (3) to assess the main environmental factors that control the phenomenon. NVC is a pristine alpine catchment in which human activity has been scarce to date. However, ARD produces striking whitish precipitates of aluminum along km-long stretches of some stream beds (Fig. 2). In recent times, signs of ARD are expanding downstream and upstream to areas where the phenomenon had not been observed during the last decades (IGC, 2012). ARD manifestations had been previously reported in the Pyrenees, but they had just seasonal development and their effects were limited to some restricted areas (e.g. Zaharescu et al., 2009; Zaharescu et al., 2016). ARD is actually becoming more widespread in several watersheds and show conspicuous manifestations regardless of the season (Figs. 1B and 2), as is the case of the NVC. This general trend leads to the hypothesis that climate (i.e. climate warming) is exerting strong control on ARD. Furthermore, some lakes and streams in the NVC headwater are acidic and show anomalous concentrations of trace metals that lead them to be qualified as polluted (IGC, 2012). In contrast, some other nearby lakes and streams are circumneutral or even markedly basic and of low metal concentrations, despite having the same elevation, orientation and bedrock mineralogy. This suggests us that, in addition to climate, other local factors may play a key role in ARD.

2. Acid rock drainage and precipitates

The weathering of sulfides is a bio-chemical process that promote the production of sulfuric acid under oxygen-rich environments (e.g. Nordstrom, 2011b). Pyrite (FeS_2) and its polymorph marcasite are commonly involved in this process, but other sulfides such as arsenopyrite (FeAsS), chalcopyrite (CuFeS_2), sphalerite (ZnS) and pyrrhotite (Fe_{1-x}S) can also take part. When exposed to air and water, the oxidation and decomposition of pyrite may produce a solution of ferrous sulfate and sulfuric acid that causes the acidification of water (reaction 1) (Bradley and Worland, 2015):



The contact with the atmosphere causes ferrous iron (Fe^{2+}) to further oxidize to ferric ion (Fe^{3+}), producing additional acidity according to the reaction (2) (Akcil and Koldas, 2006).



Depending on the specific composition of the sulfide, other minor metals (e.g. Zn, Cu, Cd, Co) and metalloids (e.g. As, Sb) may be also released in the oxidation process (Nordstrom and Alpers, 1999). The kinetics of the oxidation process is very slow, but it is typically catalyzed at low pH by the action of acidophilic archaea, bacteria (e.g. *Thiobacillus ferrooxidans* sp.) and photosynthetic algae, which increases the rate of reaction by several orders of magnitude over abiotic rates (Nordstrom and Southam, 1997; Baker and Bandfield, 2003; Jennings et al., 2008; Nordstrom, 2011b; Cruz-Hernández et al., 2012).

Al is a major component of a number of common silicate minerals and thus is a frequent element in ARD-precipitates. Al is dissolved at $\text{pH} < 4.5$ –5.6 and precipitates above this pH in the form of whitish-colored aluminum-hydroxides and -hydroxysulfates (AHPs), which composition is dependent on the bedrock mineralogy. Common aluminum-hydroxysulfates that precipitate in such pH range are aluminite ($\text{Al}_2(\text{SO}_4)(\text{OH})_4 \cdot 7\text{H}_2\text{O}$), basaluminite ($\text{Al}_4(\text{SO}_4)(\text{OH})_{10} \cdot 5\text{H}_2\text{O}$) and hydrobasaluminite ($\text{Al}_4(\text{SO}_4)(\text{OH})_{10} \cdot 12$ –36 H_2O), which is the most ubiquitous in ARD. Aluminum-hydroxides such as gibbsite (γ - $\text{Al}(\text{OH})_3$), its polymorph bayerite (α - $\text{Al}(\text{OH})_3$) and other amorphous to nano-crystalline phases are also frequent (Nordstrom and Alpers, 1999; Bigham and Nordstrom, 2000; Takeno, 2005; Sánchez-España, 2007; Sánchez-España et al., 2011; Sánchez-España et al., 2016; Gault et al., 2015).

Geochemical composition of the whitish precipitates in the NVC was determined by Igc (2012). Scanning electron microscopy with energy dispersive X-ray analysis (SEM-EDX) revealed a secondary mineral roughly cracked by dehydration, composed mainly of Al, O, and S in less quantity. The precipitates are nearly amorphous to X-ray diffraction (XRD), with just some possible nanocrystals embedded into the amorphous matrix. However, some broad reflections near 7 – 10° and 20 – 25° 2θ were recognized. This XRD pattern is compatible with aluminum secondary minerals formed at $\text{pH} \sim 4.5$ –5.0 (Sánchez-España, 2007; Du et al., 2009; Sánchez-España et al., 2011). This geochemical signature may be characteristic of aluminum-hydroxides as gibbsite or bayerite, with a minor fraction of some aluminum-hydroxysulfate as hydrobasaluminite. It should be noted that hydrobasaluminite is a metastable compound that tends to transform to a more stable phases as gibbsite or bayerite and, therefore, it is common for them to coexist (Sánchez-España et al., 2016).

3. Geological setting

The Pyrenees is a ca. 500-km long, E-W-trending mountain chain that extends between France and Spain, in SW Europe (mean latitude 42.4°N) (Fig. 1). From the geotectonic perspective, it is a double-verging thrust-and-fold belt resulting from the collision between the Iberian and Eurasian plates during the Mesozoic-Cenozoic Alpine orogeny (e.g. Choukroune and ECORS, 1989; Muñoz, 1992; García-Sansegundo, 1996). Three main structural domains are differentiated: (1) the North-Pyrenean Zone, between the Aquitanian foreland basin and the North-Pyrenean Fault, with northward verging thrust-and-fold structures involving both the Variscan basement, composed of Paleozoic rocks, and post-Variscan sedimentary successions; (2) the Axial Zone, that constitutes the core of the orogen, in which the Variscan basement forms a south-verging antiformal stack; and (3) the South-Pyrenean Zone, comprising a series of thrust sheets of Mesozoic and Paleogene formations that have been transported tectonically towards Ebro foreland basin (Fig. 1A) (e.g. Barnolas and Pujalte, 2004; Teixell and Muñoz, 2000). The Pyrenean Axial Zone is the topographically higher structural unit with a number of peaks above 3000–3400 m a.s.l.. The identified ARD

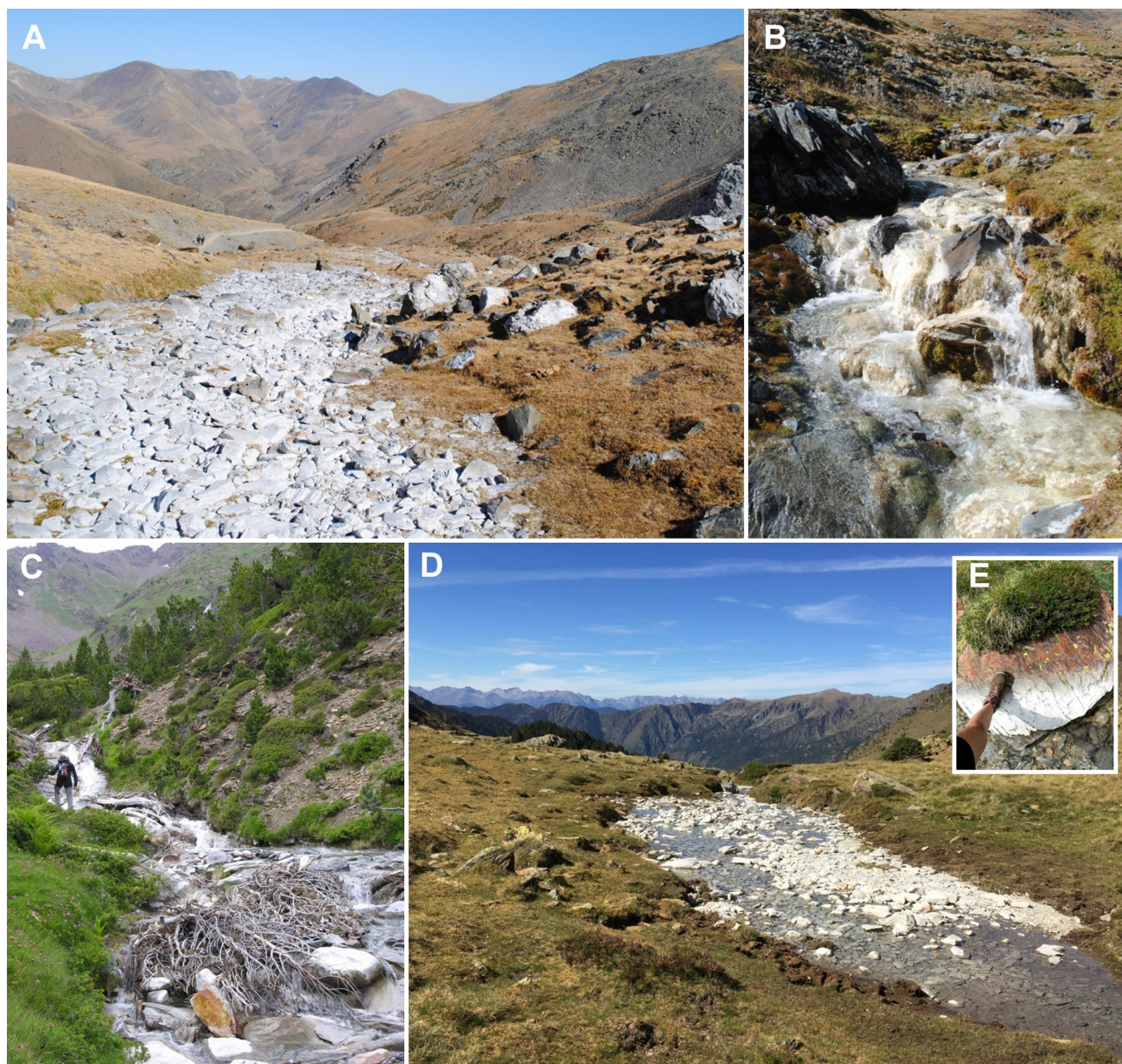


Fig. 2. Evidence of whitish aluminum-hydroxysulfate precipitates (AHPs) on stream beds in the Central and Eastern Pyrenees, at elevations ranging from 2200 to 2500 m a.s.l. (A and B) Views of two stretches of the Coma de l'Embut Creek affected by AHPs, at the Capçaleres del Ter i del Freser Natural Park (October 2017 (A) and September 2018 (B)). Note that the stream bed is white color regardless of the water flow condition. (C) Coma River, Valls del Comapedrosa Natural Park (2018). (D and E) Port Vell creek, Alt Pirineu Natural Park (September 2018).

processes occur in the Pyrenean Axial Zone, including those of the NVC analyzed in this work (Figs. 1B and 3). The exposed rocks of the Variscan basement include an intensely deformed succession ca. 2500 m thick of Paleozoic metasedimentary formations. These rocks were intruded during the late stages of the Variscan orogeny by batholiths dominated by granitoids, which developed aureoles of thermal metamorphism, in which most of the ore bodies occur.

The NVC is located within the Alt Pirineu Natural Park (Spain) (Fig. 1C). It is adjacent to the Comapedrosa Valley Natural Park (Principality of Andorra) and the Regional Natural Park of the Ariège Pyrenees (France). Here, the main structural unit is the Pallaresa anticline (Choukroune and Séguret, 1973), which affects a Paleozoic low-grade metasedimentary sequence ca. 2500 m thick (Zandvliet, 1960; Capellà and Carreras, 1996). This asymmetric anticline is offset on its northern limb by a north-dipping reverse fault system and the associated shear zone (Mérens shear zone: MSZ), which separates two different domains (Cochelin et al., 2018). Exposed rocks in the southern domain correspond

to a sequence of cm-thick beds of pelites and arenites, and sporadic m-thick quartzite layers (Alins Formation) with dominant cleavage dipping 30–60°N (Laumonier et al., 1996; Capellà and Carreras, 1996; Cochelin et al., 2018). The lithology in the northern domain is more diverse, consisting of a thick rhythmic alternation of sandstones and pelites with ferruginous beds (Sotllo Formation), intercalated microconglomerate lenticular beds, sills and felsic metavulcanites (ICGC, 2007). The dominant cleavage dips here around 60–90°N (Cochelin et al., 2018). The Al-content in the pelitic beds of the Sotllo Formation is within the 13–23% range, which is in agreement with other Cambro-Ordovician Pyrenean rocks (IGC, 2012). The N-dipping black slates and phyllites of the Lladorre Unit crop out at high elevation along a WNW-ESE strip between the Lladorre (W) and Comapedrosa (E) peaks (Fig. 1C). This 250 m thick ridge-forming formation is the most relevant in terms of ARD since it includes significant volumes of sulfide-bearing rocks (IGC, 2012).

The MSZ is associated with a 70 km-long reverse fault system with an estimated vertical displacement of ca. 2000 m. It is one of the

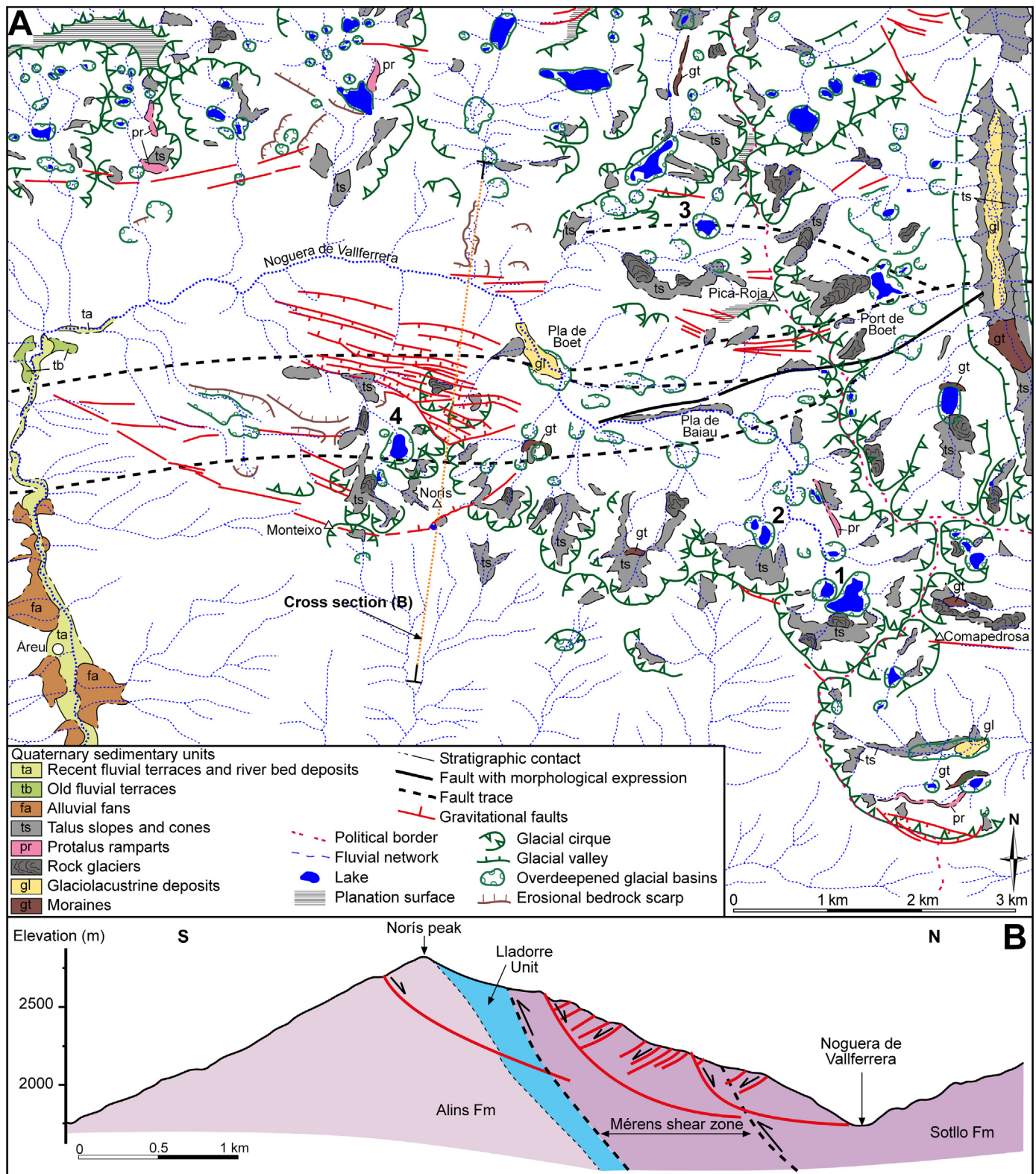


Fig. 3. Geomorphological setting of the Noguera de Vallferrera catchment (NVC). (A) Geomorphological map showing abundant periglacial and paraglacial features developed on a relict glacial landscape. Periglacial processes and gravitational slope deformation dominate in the headwaters zone. (1) Baiu Lakes, (2) Escorbes Lakes, (3) Port Vell Lakes and (4) Aixeu Lake. (B) Cross-section across the Monteixo-Noris Range showing the interpretation of a deep-seated gravitational slope deformation (DSGSD) associated with the Mérens shear zone. Note bend in the Noguera de Vallferrera stream consistent with the northward displacement of the DSGSD.

major orogen-parallel structures affecting the Variscan basement in the Axial Zone (Cochelin et al., 2018). The MSZ runs along the axial zone of the Pallaresa anticline and the northern flank of the Monteixo-Noris range. This fault-weakened zone has a conspicuous geomorphic

expression between the Baiu plain (Pla de Baiu) and the Boet mountain pass (Port de Boet) (Figs. 1C and 3). Here, the intensely sheared rocks are prone to the development of large gravitational deformations. The slopes show fresh-looking uphill- and downhill-

facing scarps up to 25 m high attributable to recent or active deep-seated gravitational slope deformation (i.e., sackung). Similar features related to gravitational faulting have been reported to the east affecting rock glaciers (Àspres de Banyell, Valira Valley, Andorra) (Turú and Planas, 2005). Both, tectonic fracturing and the recent gravitational faulting have clear implications regarding the hydrology and ARD, since they control the arrangement of the drainage network and contribute to increase the permeability of the rock massif.

Regarding the NVC landforms, glacial and periglacial features predominate above 2000 m a.s.l. (Fig. 2). Mass-wasting under periglacial conditions (e.g., frost shattering) has produced numerous deposits consisting of angular rock fragments (i.e., talus slopes and cones, rock glaciers, protalus ramparts), many of which are active in the present time. Of importance for the present study are also deep-seated gravitational slope deformations developed on oversteepened slopes carved by the glaciers and debuttressed during the deglaciation. These paraglacial features have been also reported in other sectors of the Axial Pyrenees (e.g. Gutiérrez et al., 2005, 2008, 2012; Guerrero et al., 2013; Jarman et al., 2014; McCaillin and Corominas, 2019). In the study area, these landforms display a remarkable development in the northern slope of the Monteixo-Norís range (Fig. 2). Here, the upper-middle sector of the slopes is riddled by a dense system of fresh-looking downhill- and uphill-facing scarps up to 2 km long. Some of such uphill-facing scarps affect talus slopes, suggesting that they may be currently active. These features have clear implication on the local hydrology and thus on ARD.

4. Methods

The area was investigated by integrating geological and hydro-physico-chemical data. Historical aerial photographs and orthoimages from dates spanning from 1945 to 2018 with spatial resolutions up to 25 cm/px (source: Spanish National Geographic Institute-IGN and Cartographic and Geological Institute of Catalunya-IGC) were used for geomorphological mapping and the identification of AHPs coating stream and gully beds. Particularly valuable were the aerial photographs taken in 1945–46 and 1956–57 (American flights A and B; Cartographic and Photographic Air Force Center-CECAF) that, despite their lower spatial resolution (~5 m/px and ~2 m/px, respectively), allowed us to expand the observation period to almost 75 years. The comparison between the photographs used for the analysis was possible since all they were captured during the snow-free season, ranging from the end of June to the ends of September, with the only exemption of 2009's series collected in October–November. We excluded the 2017's series from the analysis because, despite the photographs were collected at the ends of September, the land surface was partially covered by snow above 2200 m a.s.l.

AHPs signs were identified in orthoimages as stream sections with anomalous whitish colors, in contrast with the almost black appearance of the unaffected stretches (Fig. 4). The blackish tone of the unaffected sections is related to the dark color of the gravels and boulders derived from Paleozoic rocks. Infrared colored imagery captured since 1996 were also analyzed, at resolutions ranging from 2.5 m/px (1996) to 0.5 m/px (since 2008) (spectral band centered at 729.45 nm (red channel with infrared zone information), 623.82 nm (green channel with red zone information) and (543.27 nm blue channel with green zone information), source IGC). The stretches affected by AHPs are shown in infrared imagery in a color band that ranges from white or turquoise to bright blues, while the unaffected stretches are shown dark green (Fig. 4). According to these criteria, a preliminary mapping of the spatial distribution of AHPs was conducted analyzing the imagery younger than 2012. The areas were visited during 2017–2019 to corroborate the reliability of our mapping. Direct observations confirmed that AHPs are more striking during summer baseflow, but they are still visible during spring and autumn runoff, moment when the waters acquire a characteristic turquoise color (Fig. 4). In this regard, the AHPs coating gravels

and boulders lose their whitish appearance when wetted, but it is recovered moments after becoming dry. This causes the stream beds to remain whitish most of the time. It should be noted that the photographic flights are not carried out during rainy conditions. Once the preliminary mapping was validated, the AHP signs and its evolution were tracked along the complete historical series, including the lower resolution and uncolored photographs earlier than 2000 (Fig. S1 in Supplementary Material).

Sampling stations were selected according to the results of the AHPs mapping and other hydro-geomorphological criteria, in order to obtain a representative model of the entire area. A total of 68 water samples were collected from lakes, streams and seepages during three different campaigns conducted in August (Baiau and Port Vell-Pica Roja) and September (Baiau) 2018, and May 2019 (Aixeus) (Fig. 3). Samples were collected in 15 mL PP conical tubes, acidified to pH < 2 by addition of 5 M HNO₃ (ultrapure grade, Merck). The samples were preserved at T < 5–10 °C until their analysis in the laboratory. Physicochemical parameters (i.e. temperature, pH and electrical conductivity-EC) were measured at the water sampling points by a HI9810 pH-meter and HI98192 EC-meter (by HANNA), both equipped with temperature probes for enable compensation of the pH and EC values to a reference temperature of 25 °C. The meters were multiple-point recalibrated prior to each sampling campaign by certified pH-standard buffers (4.01, 7.01, 9.18, 10.01 and 12.45; ±0.01 pH at 25 °C) and EC-standard solutions (0.00, 84.01413 and 5000 µS cm⁻¹ at 25 °C).

The samples were controlled and conserved in the laboratory at a T < 5 °C. The pH of the acidized samples was checked to remain pH < 2, ultrapure HNO₃ were added if necessary, and dilution was checked prior to the lab analysis. The total concentrations of dissolved trace-metals and metalloids (Ti, Cr, Mn, Fe, Co, Ni, Cu, Zn, As, Cd, Au, Hg and Pb) were determined by inductively coupled plasma-mass spectrometry (ICP-MS) (e.g. Longerich et al., 1990; Jarvis and Jarvis, 1992) by an Agilent 7500c spectrometer. Al, major elements (Na, K and Ca), and some high-concentration trace-elements were determined by inductively coupled plasma-optical emission spectrometry (ICP-OES) by an Agilent 5100. Standard QA/QC lab protocols were observed for the analysis, including blanks and initial calibration verification by 6 to 9 different certified standards for each trace metal, continuing calibration verification every 10 samples, and dilution check. This approach enabled achieving an accuracy in the determination of the trace concentrations with limits of detection (LoD) of (Al < 5 µg/L), (Ti < 0.5 µg/L), (Cr < 0.5 µg/L), (Mn < 1 µg/L), (Fe < 6 µg/L), (Co < 0.02 µg/L), (Ni < 0.5 µg/L), (Cu < 0.01 µg/L), (Zn < 0.35 µg/L), (As < 0.2 µg/L), (Cd < 0.05 µg/L), (Au < 0.1 µg/L), (Hg < 2 µg/L), (Pb < 0.5 µg/L).

Multivariate statistical analysis was performed to better understand the correlations between pH, EC and trace metals concentrations. Covariance and correlation coefficient matrices were calculated for the sampling campaigns conducted in Baiau (summer and autumn 2018) and Port Vell-Pica Roja (summer 2018) sectors. The calculated correlation coefficients were analyzed to assess spatial and seasonal correlation patterns. The sampling conducted in Aixeus (spring 2019) was excluded from the analysis to avoid possible over interpretations.

Meteorological data was analyzed to determine temperature and precipitation anomalies. The data were registered by the autonomous meteorological stations of Vielha e Mijaran (1002 m a.s.l.) (UTM N31T 319310E 4,729,700 N), Esterri d'Àneu (950 m a.s.l.) (UTM N31T 345637E 4,721,441N), and Certascan (2400 m a.s.l.) (UTM 31T 358470E 4,728,981N) (source Meteorological Service of Catalunya, Spain). The Standardized Precipitation Index for cumulative precipitation values of 12 months (SPI12) (McKee et al., 1993) was computed by the SPI Generator software (National Drought Mitigation Center - UNL) for the historical period 1955–2017, according to the meteorological data recorded by the Esterri d'Àneu meteorological station.

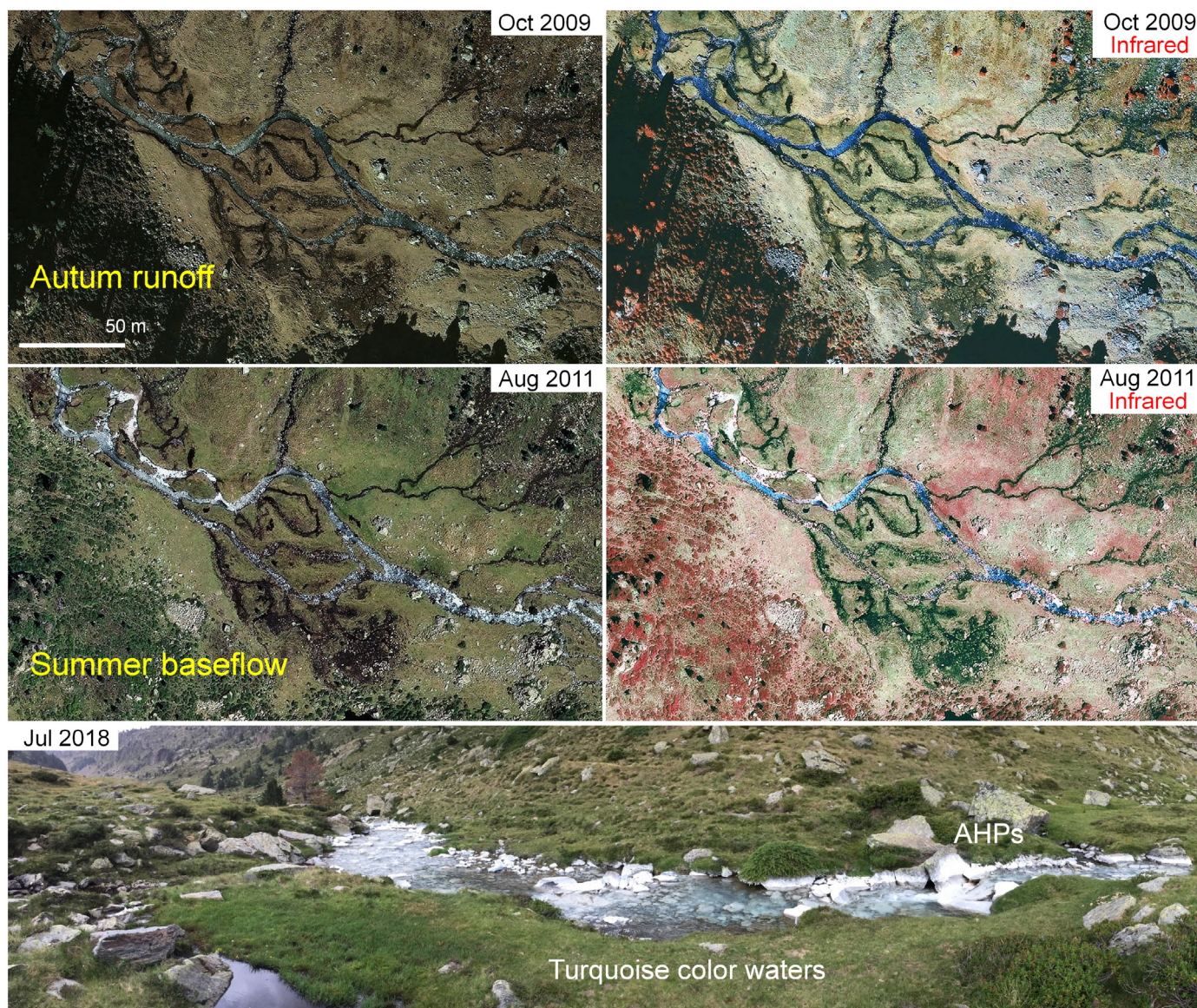


Fig. 4. Historical true-color and infrared aerial orthoimages of a stretch of the Baiau River at the Pla de Baiau plain (2170–2175 m a.s.l., centered at WGS84 UTM N31T 370220E 4,718,950 N), captured during wet (October-2009) and dry (August-2011) seasons (source Cartographic and Geological Institute of Catalunya-ICGC, Spain). Stream waters depict different color pattern depending on whether they are affected or unaffected by aluminum-precipitates (AHPs), regardless of the flow regimen. Affected waters appear turquoise in true-color and bright blue in infrared imagery, while unaffected waters look black (true-color) or dark green (infrared). Bottom photography, panoramic view of a section of the Baiau River upstream the Pla de Baiau (UTM N31T 370630E 4,718,325N; see location in Fig. 6). Note the turquoise color of the stream waters, characteristic of the rivers affected by AHPs.

5. Results

5.1. Hydrochemistry and geochemistry

The water samples were classified into three groups according to their pH: acidic ($\text{pH} < 5.6$), circumneutral to basic (hereinafter so called “non-acidic”) ($\text{pH} > 6.5$) and water mixes ($5.6 < \text{pH} < 6.5$) (Fig. 5 and Table S1 in supplementary material). The acidic waters (i.e., lakes, streams and seeps) are ascribed to locally recharged groundwater that has flowed through sulfide-rich rocks or deposits and are altered by ARD. Some lakes in the NVC headwaters as e.g. Baiau Lakes at 2480 m a.s.l. ($\text{pH} \sim 4.7$) and Aixeus Lake ($\text{pH} \sim 4.9$) at 2365 m a.s.l. (labeled as 1 and 4 in Fig. 3) are among the most acidic ones in the Pyrenees (Catalan et al., 1993; Pla, 2001; Jean-Christophe Auguet and Casamayor, 2013). Such lakes are fed by acidic and non-acidic seepages that supply inflows throughout the year, in addition to surface runoff, including snow melt and direct rainfall. The acidic gullies and streams are sourced by acidic

seepages and lake outlets and maintain their condition until they converge with non-acidic ones. Some acidic springs and seepages are at elevations as low as 1860 m a.s.l. (Mossen Batlle; $\text{pH} \sim 4.8$), 1650 m a.s.l. (seepage at the foot of Monteixo peak; $\text{pH} \sim 5.4$) and 1220 m a.s.l. (Areu village spring; $\text{pH} \sim 5.6$). Non-acidic waters are the most abundant in the NVC. For instance, Escorbes lakes at 2374 m a.s.l. ($8.2 < \text{pH} < 10.1$) and Port Vell lake at 2465 m a.s.l. ($\text{pH} \sim 9.5$) (labeled as 2 and 3 in Fig. 3), and the majority of the streams and creeks, with pH values typically within the 6.5–9.5 range. These are essentially surface waters that had none or limited subsurface circulation. Water mixes result from the mixing at the surface of acidic and non-acidic waters. The mixing mostly initiates below 2500 m a.s.l. (e.g. Baiau cirque-Portvell, 2470 m a.s.l.; Port Vell-Pica Roja sector, 2480 m a.s.l.) (Figs. 6 and 7).

Water samples have low electrical conductivity ($\text{EC} \sim 9$ to $326 \mu\text{Scm}^{-1}$) as expected for low-mineralized mountain waters (Fig. 5 and Table S1 in supplementary material). EC is higher in late summer (post-thaw baseflow) than in autumn (rainy season) and acidic waters

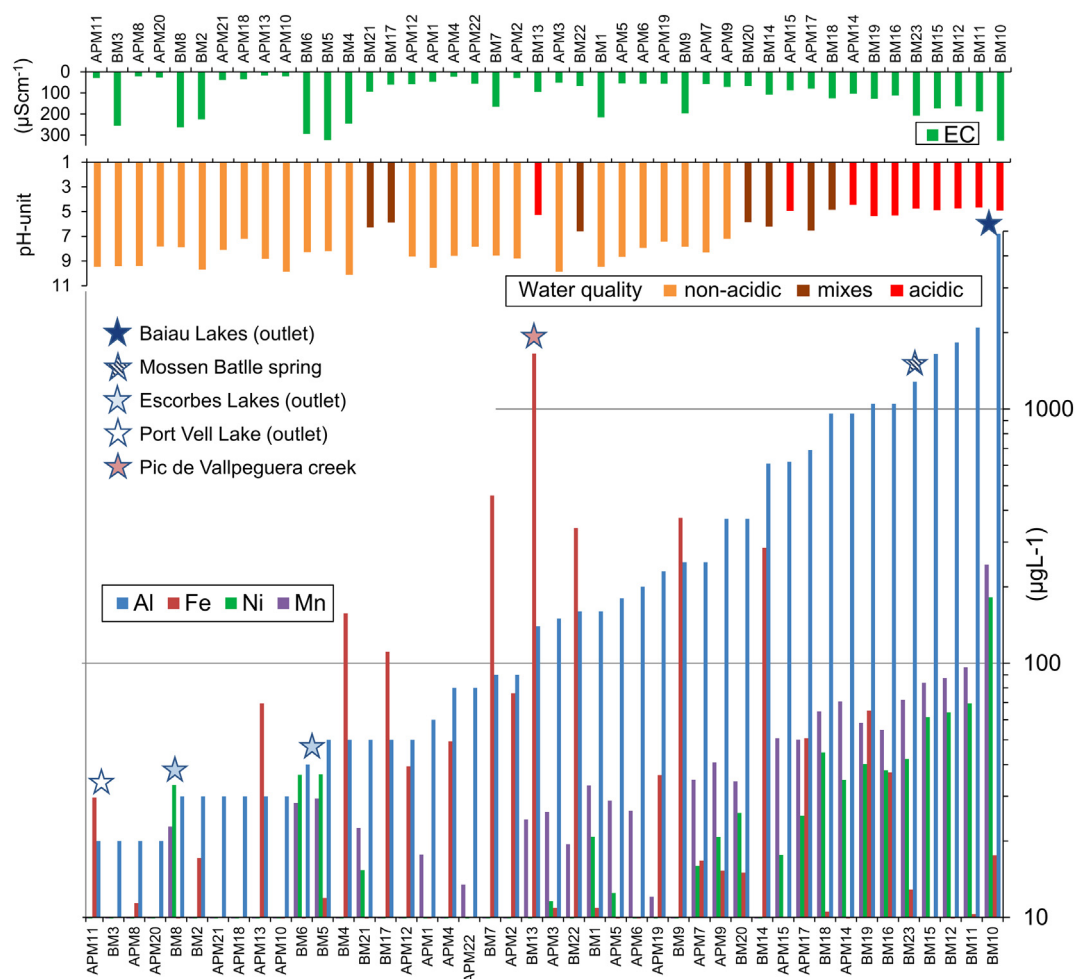


Fig. 5. Physico-chemical features of the water samples collected during the summer of 2018 in the Baiau (labeled as BM-) and Port Vell-Pica Roja sectors (labeled as APM-) (see additional data in Table 1 in supplementary material). Three water types are distinguished: acidic (pH < 5.6, enriched in metals), non-acidic (pH > 6.5, non-enriched in metals) and water mixes (pH ~ 5.6–6.5). Note the marked differences in the water quality of the nearby Escorbes (2370 m a.s.l.) and Baiau (2480 m a.s.l.) lakes (Fig. 7B), despite their similar elevation and orientation on the north-facing side of the ridge, and bedrock lithology.

generally have higher EC than the non-acidic ones, although with a difference below one order of magnitude. EC is also above the average ($\bar{X}_{EC} + \sigma$) in the non-acidic Escorbes Lakes, and in the lower part of the catchment (Pla de Boet). More significant are differences in terms of metal concentrations, exceeding two orders of magnitude ($\times 500$) in creeks located just a few meters away, despite the mineralogy of the substrate in its headwaters is the same. The most relevant differences correspond to the aluminum-ion, ranging from <10 to 4890 $\mu\text{g/L-Al}$. Overall, the concentration of minor- and trace-metals are higher in acidic waters, especially aluminum that shows the broadest concentration range (Fig. 5 and Table S1 in supplementary material). Aluminum, manganese, cobalt, zinc, copper, and cadmium concentrations show good correlation with acidity, regardless the location or the season (Fig. 8). For example, the maximum aluminum-concentrations (>2000 $\mu\text{g/L}$) are reached at pH < 4.9 (with the sole exception of one sample at pH ~ 5.2). More disparity is on the concentrations of the other trace metals lead, titanium, arsenic, gold, and mercury regarding the pH. In the case of nickel, high concentrations (>30 $\mu\text{g/L-Ni}$) are in acidic waters, but also in the non-acidic waters of the Escorbes Lakes (33–37 $\mu\text{g/L-Ni}$ at pH = 7.9–8.3). A particular pattern is observed for the iron-concentration, suggesting that aluminum and iron may have different ARD behavior –iron is found at high concentrations in a higher pH range, with the majority of concentrations >100 $\mu\text{g/L-Fe}$ reached at pH > 6.

Regarding the aluminum precipitation, aluminum comes from the chemical weathering of feldspars and phyllosilicates present in the siliciclastic metasedimentary bedrock (e.g. micas, albite, orthoclase).

Al mainly occurs as Al^{3+} (aq) in acidic waters (pH < 5.0–5.6) (e.g. Takeno, 2005), but where they mixes with non-acidic waters, the acidity of the former is buffered, and the conditions for Al precipitation are reached, typically in the form of whitish AHPs. The precipitation of the AHPs in the NVC roughly initiate around 2400–2500 m a.s.l. and extends down to ca. 1800–1700 m a.s.l.. As an example, ephemeral AHPs start to occur at ca. 200 m (2420 m a.s.l.) downstream the small Baiau Lake outlet (2480 m a.s.l.), (Figs. 6 and 7). AHPs form where the acidic waters converge and start mixing with creeks of non-acidic waters, flowing from the slopes on both margins of the Baiau river. Progressive mixing causes AHPs to grade downstream from ephemeral to discontinuous and become clearly continuous just downstream of the junction with the Escorbes creek (2325 m a.s.l.). AHPs also become discontinuous, but still evident from the Pla de Baiau (2170 m a.s.l.) down to the Boet plain (Pla de Boet) (1800 m a.s.l.) (Fig. 7B). Analogous patterns have been observed in the Port Vell – Areste creeks (Fig. 7A), where AHPs initiate at 2530 m a.s.l., Sotllo creek (at 2450 m a.s.l.), Medacorba and Barèitas rivers (at 2300 m a.s.l.), Vallpeguera creek (at 2510 m), and Gardelha river (at 2580 m a.s.l.) (Fig. 9). The total length of affected stream stretches exceeded 35 km in 2018.

5.2. Spatial-temporal patterns of ARD during the period 1945–2018

A detailed analysis of the spatial-temporal distribution of the AHPs using the 1945 to 2018 historical orthoimages reveals that the extent of the affected areas has changed considerably throughout the past

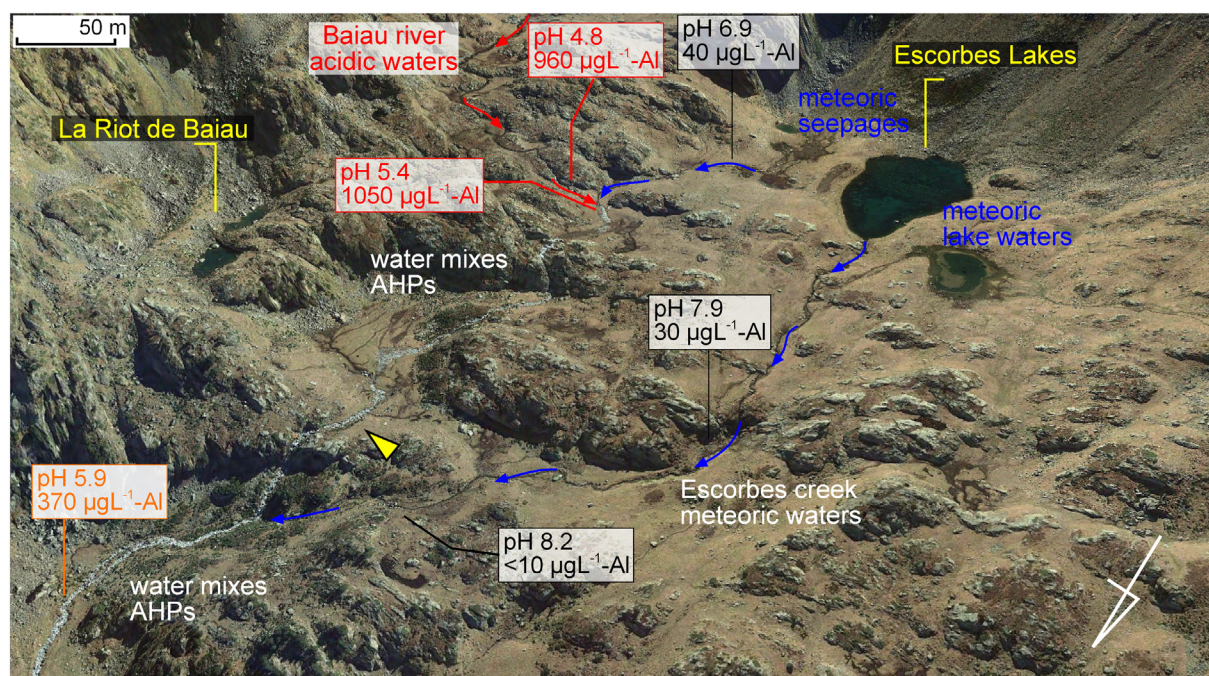


Fig. 6. Water mixing downstream of the Baiau lakes (pH 4.9; $4890 \mu\text{g L}^{-1}\text{-Al}$). Aluminum-hydroxysulfates precipitation (AHPs) occurs in areas where the acidic Baiau River (Aluminum-enriched) converge with the meteoric Escorbes creek. Yellow arrow indicates the position of the panoramic view in Fig. 4. White arrow points to N (oblique view from Google Earth, centered in YTM 31 T 370320E 4,718,200 N).

decades (Figs. 9 and S1 on supplementary material). Signs of AHPs were already observable in the American flights from 1945 to 46 and 1956–57, respectively. AHPs affected the Areste and Port Vell creeks from 2380 m a.s.l., and the Arcalís creek down to 1890 m a.s.l.. The images suggest that AHPs were continuous in the Port Vell-Areste creeks, while they were dim and intermittent in the Arcalís creek. Evidence of AHPs were also observable in the Noguera de Vallferrera river, ceasing at ca. 1 km downstream the confluence of the Port Vell-Areste and Arcalís creeks (ca. 1700 m a.s.l.). AHPs were most likely already present before 1945, at least on the northern edge of the NVC. The local names of some affected areas in the French eastern slope such as Étang Rouge (red lake) and Riou Blanc (white river) (Fig. 9) indicate that the phenomenon must have been frequent since ancient times. Noticeable is that the total length of affected streams in 1945–46 were just around 5.1 km, and that no AHPs were observable above 2380 m a.s.l. in the Areste-Port Vell creeks and above 2150 m a.s.l. in the Vallpeguera creek, which are elevations 200 to 360 m lower than the current maximum elevation of the AHPs in the same areas.

Time-lapse historical series since 1945–46 allow tracking the evolution of the AHPs up to the present (Fig. 9). No significant differences are observed in the 1956 images, compared to those of the previous decade. Nevertheless, the images younger than 1956 show an overall expansion trend, both in the total affected lengths and in the elevation at which the AHPs initiate. The AHPs expansion was not constant over time, but show peaks in 1997–98, 2007, and a maximum in 2012. In 1997–98, AHPs extended along the Noguera de Vallferrera river downstream to the confluence with the Sotillo creek, and affected D'Aixeus and Mercat creeks for the first time, from elevations of 2350 and 2180 m a.s.l., respectively. In 2007, AHPs spread to the streams located on the slopes south of Pla de Boet and Pla de Baiau (up to 2150 m a.s.l.) and north (2350 m a.s.l.) of Pla de Baiau. AHPs covered drainage sections with a total length of 38.3 km in 2012, which is the maximum for the whole record period; and the AHPs elevation scaled up to 2300–2580 m a.s.l. in all the catchments (Table S2 in supplementary material). AHPs have continued to be widespread during the following period (2013–2018), but their extent and maximum elevation have not exceeded the maximum recorded in 2012.

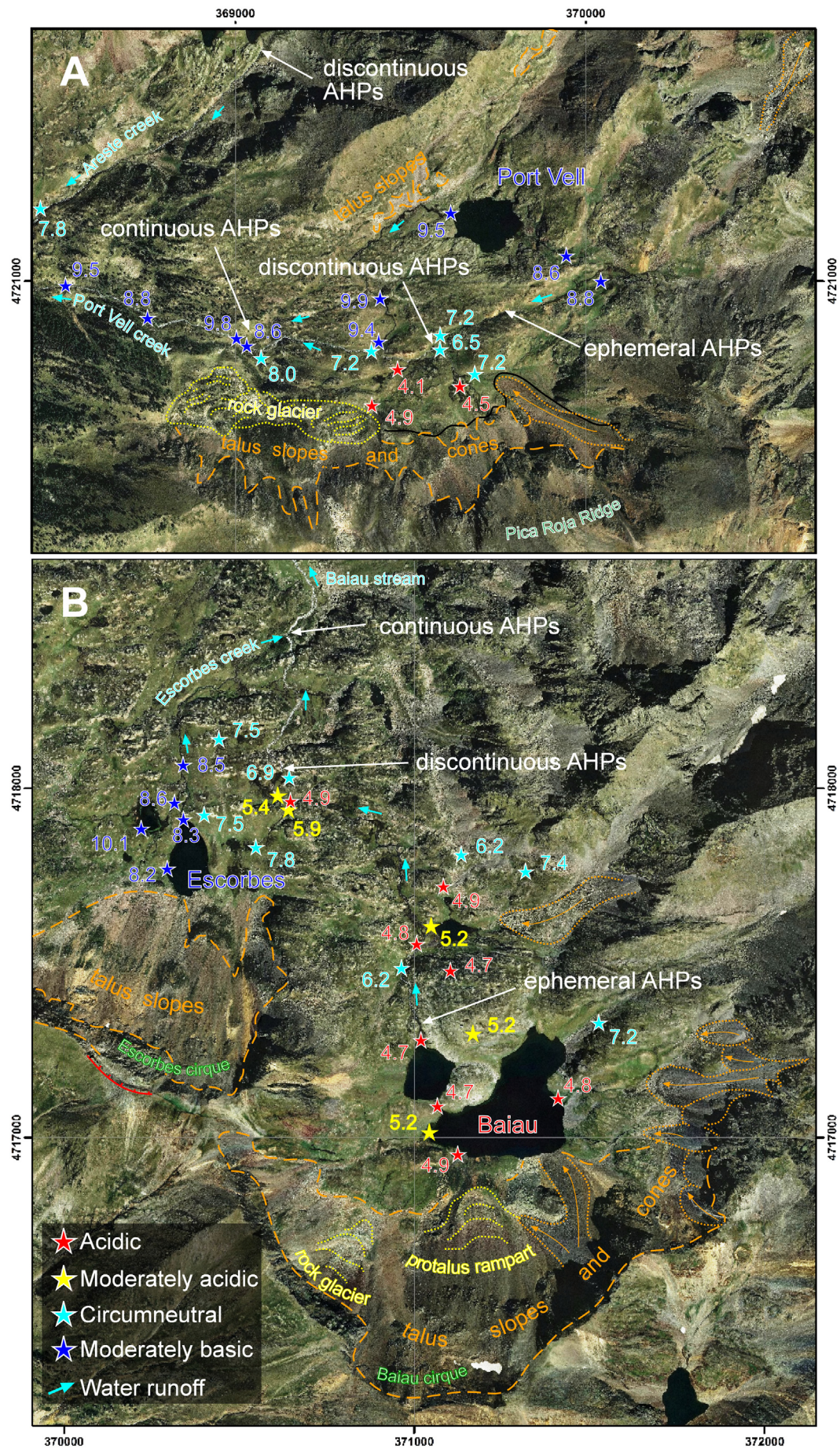
5.3. Temperature and precipitation anomalies

Temperature anomalies have been observed in the local meteorological stations of Vielha e Mijaran (1002 m a.s.l.), Esterri d'Àneu (950 m a.s.l.) and Certascan (2400 m a.s.l.), located respectively 50 km-W, 30 km-W and 15 km-NNW from the NVC (source Meteorological Service of Catalunya) (Figs. 10 and 11). A rough positive mean annual temperature (T_{mean}) trend of ca. $+0.36^\circ\text{C/decade}$ was recorded in Vielha e Mijaran station since 1980, while for 1955–1979 it was negative ($-0.04^\circ\text{C/decade}$) (Fig. 10). The warmest years were 1997, 2006 and 2011, with (T_{mean}) exceeding $+1.8\sigma$ the average value (\bar{X}_T), and 2014–2016, during which (T_{mean}) was constantly above ($\bar{X}_T + 1.6\sigma$). Regarding precipitation anomalies, the standard precipitation Index for cumulative precipitation values of 12 months (SPI12) computed for the historical period 1955–2017 (Esterri d'Àneu station data) reveals that severe to extreme ($-1.5 < \text{SPI12} < -2.5$) and exceptional ($\text{SPI12} > -2.5$) droughts were rare between 1955 and 1980, while they have been frequent in the last 3 decades, being especially noticeable the one that preceded 2012 (Fig. 10).

6. Discussion

6.1. Trace metals in waters

Chemical analysis of waters reveals that, in some areas of the NVC, concentrations for potentially toxic trace metals such as Al, Cd, Co, Cu, Ni or Zn largely exceed quality standards for aquatic ecosystems (e.g. GBC, 2018) and drinking-water laws (e.g. World Health Organization (WHO); U.S. Environmental Protection Agency (EPA); Directive 98/83/CE). Some spatial and temporal patterns regarding pH, EH and trace metals concentrations correlations are also observed (Fig. 8). The correlations between trace metals and acidity and EC are higher in Port Vell-Pica Roja than in Baiau sectors. The correlations in Baiau are higher in summer than in autumn. The correlations with EC are moderate to low in Baiau, while they are high in Port Vell-Pica Roja. Differences between Port Vell-Pica Roja and Baiau likely are because the acidic streams



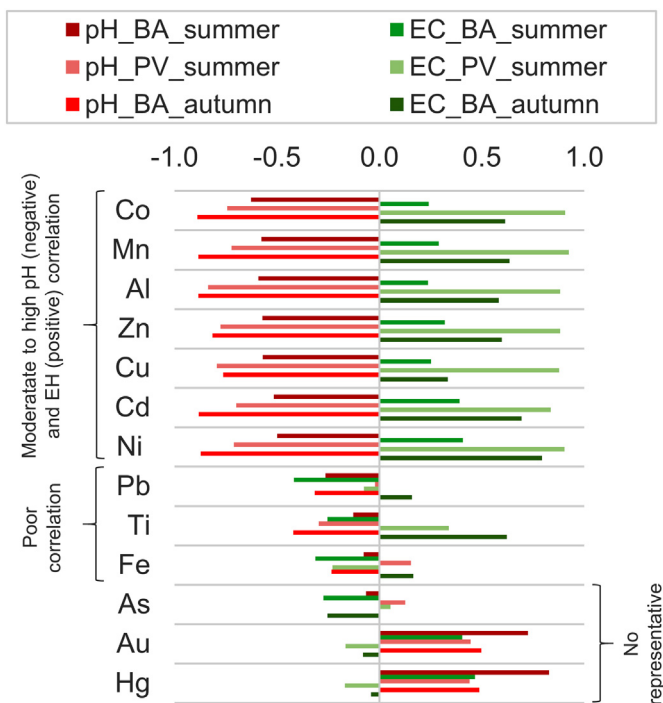


Fig. 8. Multivariate correlation coefficients of the correlations between pH - electrical conductivity (EC) and concentration of trace metals, for the campaigns conducted in Baiaú (BA) and Port Vell-Pica Roja (PV) sectors in summer and autumn 2019.

in Port Vell-Pica Roja are recharged by acidic seepages discharging from the Pica Roja slopes (Fig. 7A); while in Baiaú, acidic waters are both in lakes as in streams, which are sourced by the Baiaú lakes' outlets (Fig. 7B). More uncertainty is regarding the seasonal pattern observed in Baiaú. Here, the correlation with trace metals is lower in summer than in autumn, despite acidity and EC are higher in summer, indicating lower dilution of waters altered by ARD during the dry season. It should be noted that the summer campaign was a bit more extensive than the autumn campaign, which hampered the direct comparison (Fig. 5 and Table S1 in supplementary material); and only two campaigns do not seem sufficient to conduct a rigorous statistical analysis. Moreover, in addition to pH and EC variation, other processes can influence the correlations such as biological activity and flow regimen. Thus, the observed correlations should be taken with caution and only general trends be considered. Further research is required to better understand the distribution of dissolved trace metals and their seasonal patterns, which are key aspects to take into account for a correct management of this hydro-environmental problem.

6.2. Climatic control

The results point towards ARD processes has become more widespread and severe in the NVC in recent decades. This hypothesis has been verified since 2005 by direct observations (IGC, 2012), and it has also been supported by the space-time analysis of the 1945–2018 historical aerial imagery. We are aware on the limitations of this approach, especially were the analysis based on the lower-resolution and uncolored orthoimages younger to 2000. However, extending the observation beyond 2000, although it partially compromises the resolution, has the potential to offer a more representative longer-term diagnosis.

It should be noted that the analysis of the higher-resolution colored images, coupled with the infrared images, has offered very consistent results when compared with the infield mapping observations. Furthermore, such observations are also consistent with the climatic patterns recorded instrumentally during the same time span, and a relationship between the local effects of climate warming (i.e. temperature increasing and variation in the precipitation regimen) and the ARD aggravation can be established. In this regard, one of the most critical periods to support our analysis, such as the period 2007–2012, is covered by high-resolution colored and infrared imagery. This leads us considering the interpretations for the entire period as reasonable approximations. On the other hand, this approach attempts providing information that would not otherwise be possible, considering the gap of knowledge on historical water quality data in areas where, as in the NVC, no controls have been carried out in the past due to its remoteness.

The results also indicate that the acidification and metal enrichment of the analyzed waters are essentially caused by natural ARD processes in the NVC. AMD does not seem to be a likely origin because, although extensive mining activities have been carried out in the Vallferrera area in the past, to our knowledge extraction sites were always at elevations below 2400–2500 m a.s.l.. Some atmospheric contribution of airborne metals, either anthropogenic or natural, cannot be ruled out (Bacardit and Camarero, 2009; Camarero et al., 2009a; Camarero et al., 2017; Corella et al., 2017, 2018). However, the fact that different water masses in the same area show highly heterogeneous metal concentrations (e.g. Baiaú vs. Escorbes and Port Vell lakes) point to the potential atmospheric input is very limited compared to the geogenic contribution. The elevated metal concentrations recorded in the area also corroborates it. Thus, the projections that foresee a progressive acidification recovery of the surface waters due to the decrease in industrial activity, which peaked during the 1960s to 1980s in this region (e.g. Camarero et al., 2009b), are not applicable in the high-elevation NVC.

Climate has been invoked to exert a strong control on ARD (Furniss et al., 1999; Plumlee et al., 1999), and climate warming to be the cause of recent water quality deterioration in high-mountain areas worldwide (Nordstrom, 2009; Todd et al., 2012; Manning et al., 2013; Ilyashuk et al., 2014, 2018; Zaharescu et al., 2016). Variations in precipitation and temperature have several effects on ARD. On the one hand, a decrease in precipitation amount may cause (a) less dilution of solute-rich flows that feed streams and lakes; and (b) increasing of the fresh rock surface exposed to oxidation due to water table decline. On the other hand, an increase in air temperature causes (c) a reduction in snow and ice covers; (d) ground-ice thawing from permafrost, including detrital glacial and periglacial deposits (e.g. moraines, rock glaciers, talus slopes), which have been related to ARD (Williams et al., 2006; Todd et al., 2012); and (e) an acceleration of sulfide bio-chemical oxidation due to its positive correlation with temperature (Ahonen and Tuovinen, 1991; Schoonen et al., 2000), especially in the case of the oxidizing action of acidophilic archaea, bacteria, and photosynthetic algae (Baker and Bandfield, 2003; Nordstrom, 2011a; Cruz-Hernández et al., 2012). Furthermore, once triggered, sulfide oxidation is an extremely exothermic reaction that can elevate sufficiently the temperature on the groundwater-ore oxidation interphase even at low temperatures, making oxidation processes even more efficient (Bigham and Nordstrom, 2000; Gault et al., 2015).

The main AHPs peaks in the NVC occurred in 1998, 2007 and 2012, being the latter the most pronounced one to date. Noteworthy correlations between the temporal AHP peaks and sharp precipitation and temperature anomalies may be established (Figs. 10 and 11). This supports that the recent warmer and dryer conditions have enhanced ARD processes. Systematic positive trends in temperature (T_{\max} =

Fig. 7. Geomorphological features and signs of Aluminum-hydroxysulfates precipitation (AHP) in the (A) Port Vell-Pica Roja and (B) Baiaú sectors (UTM N31T). Acid and moderately-acid waters ($\text{pH} < 5.6$) are derived from the Pica Roja slopes and the acidic Baiaú lakes. AHPs initiate downstream of the acidic Pica Roja seepages and Baiaú lakes and change from ephemeral to continuous in the Port Vell creek and downstream of the confluence between the Baiaú river and the Escorbes creek. Acidic waters drain from the north-facing slopes of the Pica Roja ridge and the Baiaú cirque, with extensive periglacial deposits, while waters from the Port Vell and Escorbes lakes areas, with less abundant periglacial deposits, are circumneutral to moderately basic, supporting a geomorphological control on AHPs.

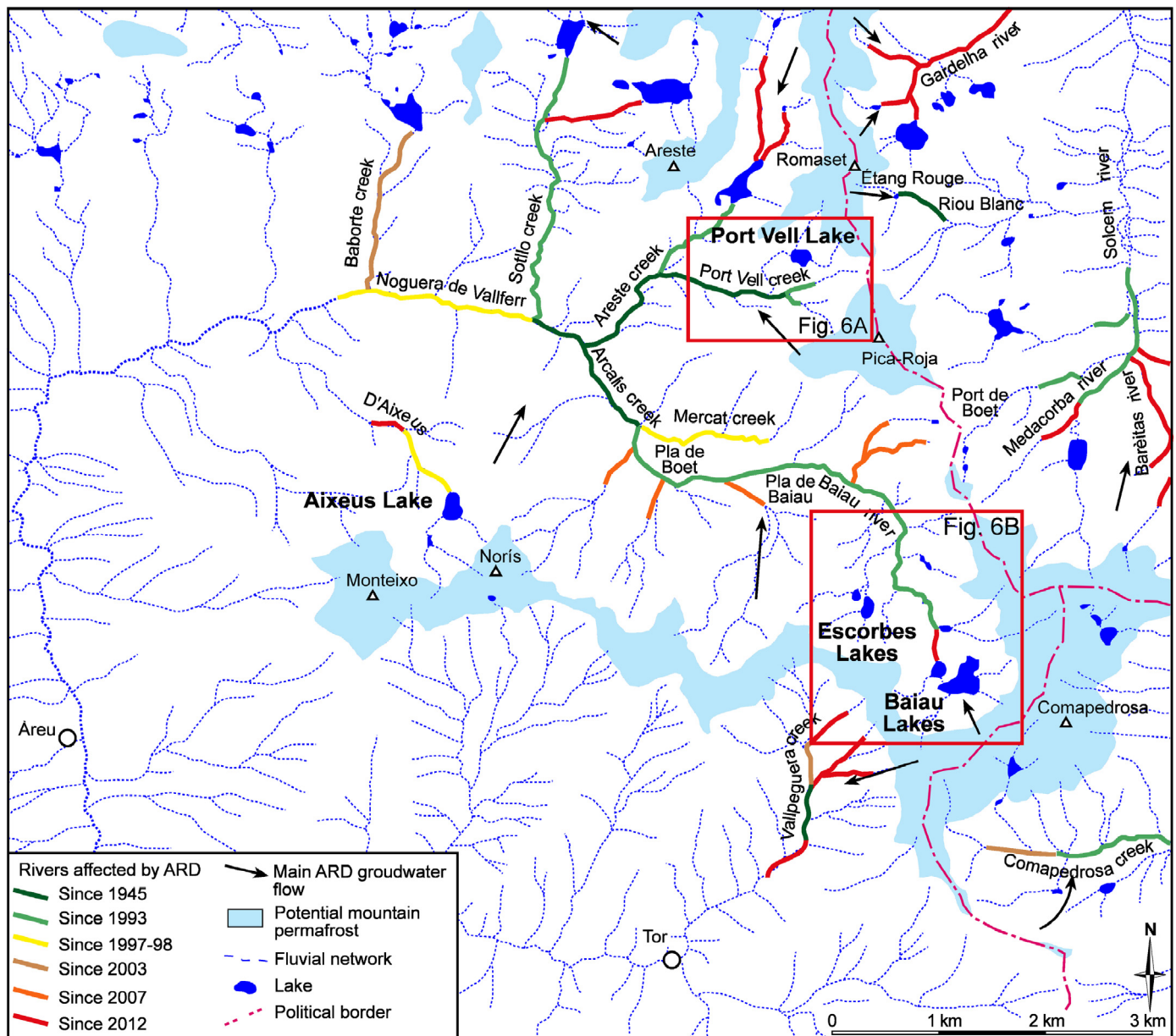


Fig. 9. Map showing the temporal (1945 to 2018) and spatial evolution of the areas affected by natural Aluminum-compounds precipitation (AHP) in the Noguera de Vallferrera catchment (NVC). The temporal pattern indicates that AHPs have significantly spread since 90s, with precipitation peaks in 1997–98, 2007 and a maximum in 2012. The total length of affected streams and creeks has increased from ca. 5 km (1945–56) to 38.3 km (2012). Noticeable is that the elevations at which AHPs initiate have climbed ca. 100 to 400 m, reaching up to 2580 m a.s.l., which matches with the elevation of the potential mountain permafrost limit in the Pyrenees (Serrano et al., 2009; Oliva et al., 2016).

+0.57 °C/decade; T_{\min} = +0.23 °C/decade) and less significant negative precipitation trends (ca. −3%/decade to −5%/decade), with greater dispersion along the mountain range, have been identified in the central Pyrenees since the 1970s–1980s (Pérez-Zanón et al., 2017; OPCC-CTP, 2018). Similar temperature anomalies have been observed in the local meteorological stations of Vielha e Mijaran (1002 m a.s.l.), Esterri d'Àneu (950 m a.s.l.) and Certascan (2400 m a.s.l.), which may be reasonably representative of the climate in NVC. Vielha e Mijaran is the only station with a long temperature dataset (1955–2018), covering almost the entire time span of the historical orthoimages (Fig. 10). The rough positive mean annual temperature (T_{mean}) trend of ca. +0.36 °C/decade recorded since 1980 exceeds in 30% the world average (OPCC-CTP, 2018). Noticeable is that the 1998, 2007 and 2012 AHP peaks occurred after the warmest years of the record period 1997, 2006 and 2011 (Figs. 10 and S1 in supplementary material).

In addition to thermal anomalies, AHP peaks also occurred after precipitation negative anomalies. The SPI12 calculated from the Esterri d'Àneu station data for the historical period 1955–2017 reveals that severe to extreme and exceptional droughts have been more frequent in the last 3 decades. All AHP peaks occurred within the dry period (Fig. 10). The more local, but shorter precipitation data from Certascan station also confirm that a drought period preceded the 2007 peak (Fig. 11), but this is not so evident for the 2012's peak, the most intense event observed to date. While at regional scale the period 2010–2012 was exceptionally dry (Fig. 10), it was not as dry in the NVC (Fig. 11). However, it highlights that the highest thermal anomaly (+0.8 °C), only exceeded in 2015, and the maximum thermal amplitude ($T_{\text{max}} - T_{\text{min}}$) was in 2012 (47.4 °C). It suggests that both low precipitation and high temperature aggravate ARD, but once triggered, temperature is probably the main catalyzer for the phenomenon. This hypothesis also supports why chemically unstable compounds such as AHPs are still very patent

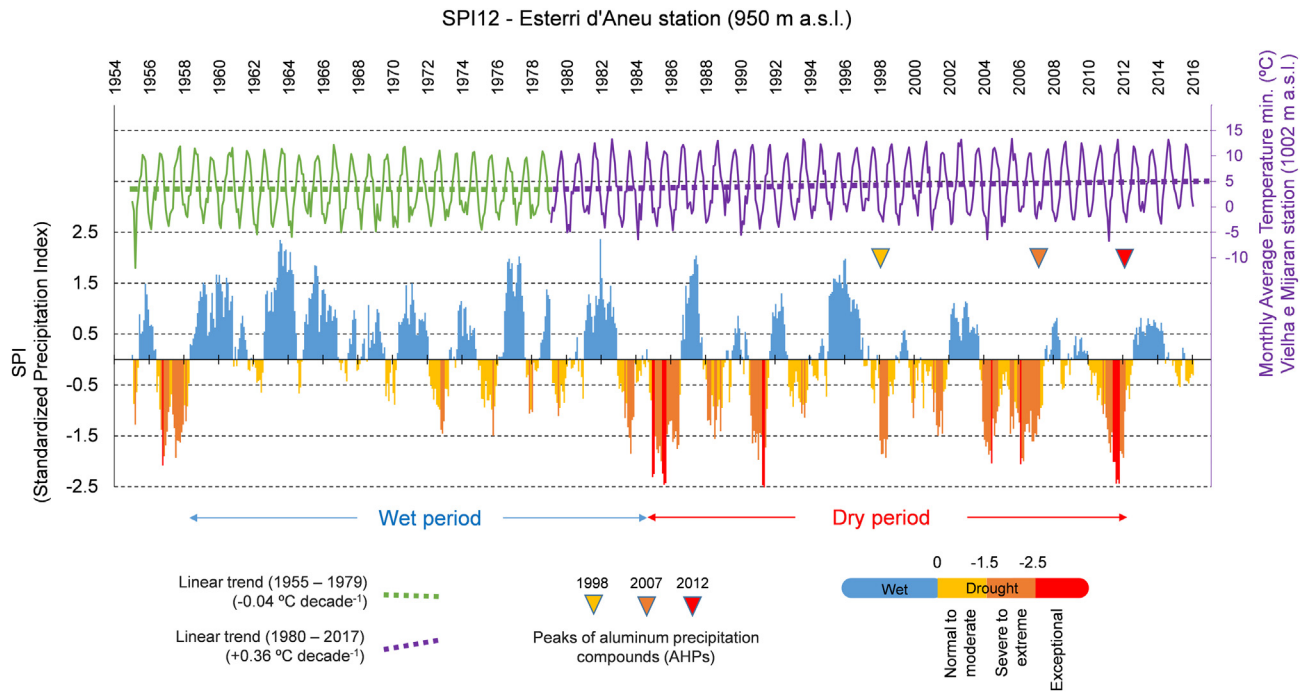


Fig. 10. Standardized Precipitation Index for a time-scale of 12 months (SPI12) for the period 1955–2017 based on the meteorological data collected at the Esterrí d'Aneu station (UTM N31T 345637E 4,721,441N), and monthly average minimum temperature (T_{\min}) at the Vielha station (UTM N31T 319310E 4,729,700N) for the same period (source: Meteorological Service of Catalunya). A change in trend both in precipitation (negative) and temperature (positive) is observed since 1980s. The main Aluminum precipitation (AHPs) peaks detected in the Noguera de Vallferrera Catchment (NVC) occur after drought periods, and especially high-temperature episodes.

despite precipitation has increased largely since 2012 (e.g. SPI24 for Sep-2017 to Sep-2019 was $> +3$, source: Meteorological Service of Catalunya). A likely cause is that above-average temperatures were more common in recent years and the average temperature stands up on historical maximums of the last hundred years (OPCC-CTP, 2018).

6.3. Elevation-dependent warming and elevation range of ARD

Results also suggest that climate warming plays some role in the expansion of the elevation range at which ARD occurs. We postulate that the rise in elevation of the edge of the periglacial and permafrost realms

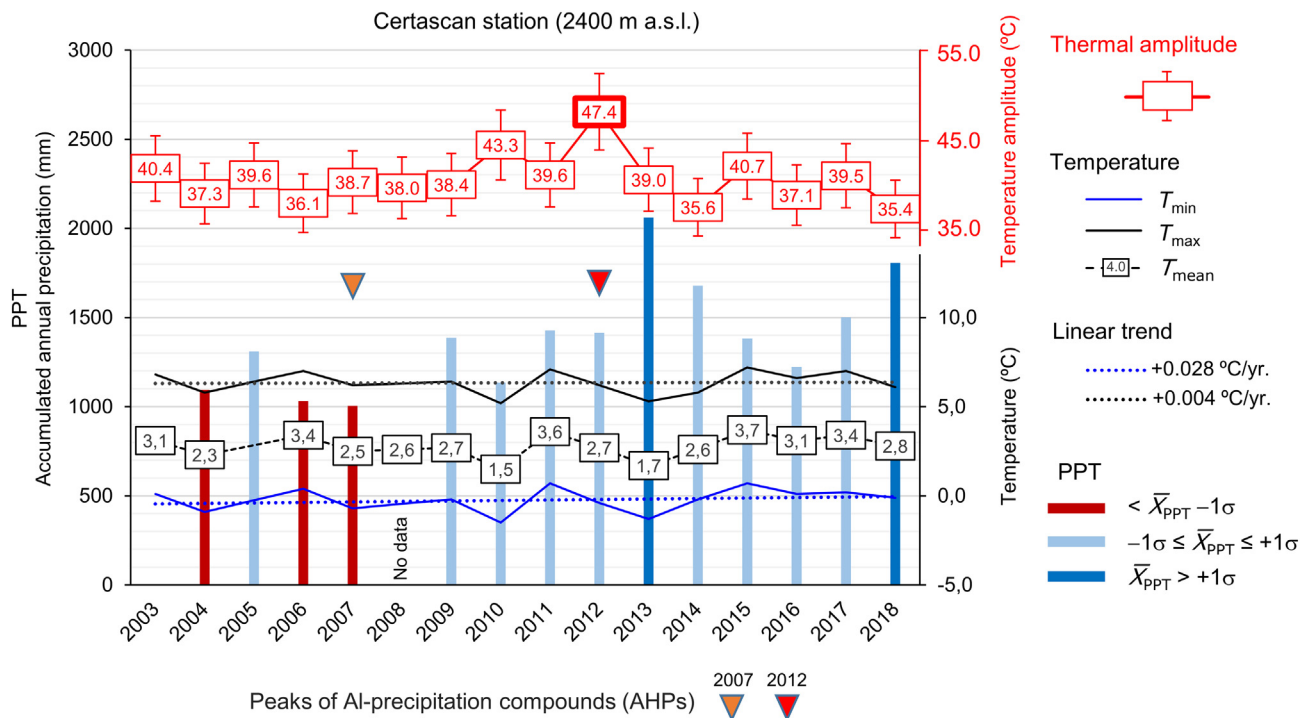


Fig. 11. Meteorological data for the period 2003–18 from Certascan automated station (15 km-NNW away from the Noguera de Vallferrera Catchment, UTM 31T 358470E 4,728,981N) (source Meteorological Service of Catalunya). The graph shows a good correlation between the low-precipitation period of 2003–2007 and the Aluminum-precipitation (AHPs) peak in 2007. The relationship with precipitation in the case of the 2012-peak is not as clear, while it coincides with a thermal amplitude peak. Note also that the average temperature in the 2011 is almost the maxima of the instrumental record.

is the main cause of the upward expansion of the AHPs in the NVC in recent decades. Here, the presence and extent of the permafrost is not well documented. However, based on geomorphological indicators and temperature data, the existence of permafrost above 2500–2700 m a.s.l. is plausible in this area (Serrano et al., 2009; Oliva et al., 2016), especially in the north-facing slopes of the Monteixo-Norís, Comapedrosa, Pica Roja and Areste peaks (Fig. 9). Noticeable is that the most acidic waters occur in the Baiau Cirque, Port Vell-Areste and Aixeus areas, where surface waters are sourced from the slopes of these peaks with a dominant north aspect.

Climate warming is accelerating changes in the hydrological and cryospheric dynamics in alpine catchments (Pepin et al., 2015). One of the most relevant effects of the elevation-dependent warming is that glacial and periglacial boundaries are retreating dramatically in the last few decades. Generally, where mean annual air temperatures (MAAT) remain below +3 °C, ground ice and permafrost are expected to persist for some periods throughout the year, which is considered as a periglacial environment (French, 2011, 2018). In areas where MAAT remains below −2 °C, groundwater persists as ground ice, which causes Fe²⁺ biochemical oxidation to slow down and oxygen available for the reaction to drop severely. Conversely, in periglacial belts where MAAT ranges between −2 °C and +3 °C, the moisture and oxygenation conditions of the rock massif vary throughout the year, allowing sulfide oxidation (Ilyashuk et al., 2018). The MAAT recorded by the Certascan automated weather station ranged between +1.5 and +3.7 °C during the period 2003 to 2018, with an average of +2.8 °C ($\sigma = 0.6$ °C). This means that the periglacial limit is located within the elevation range of ca. 2400 to 2600 m a.s.l.. Note that 10.5 km² of the study area are situated above 2600 m a.s.l., which is almost the 10% of the total.

The average rising rate of the AHPs upper limit observed in the Areste, Baiau, Vallpeguera and Sotillo creeks over the 1945–2012 period is around 50–60 m/decade, and 45–55 m/decade extending the period to 2018. Although we are aware of the significant limitations of the data derived from the interpretation of the historical orthoimages, the observed general trends are quite consistent for the different catchments, supporting that they may provide a reasonable approximation to the phenomenon. In this sense, noteworthy is that the rising rates are closely in agreement with the rise of the 0 °C isotherm estimated for the region at 46 m/decade, considering a temperature rise of ca. 0.23 °C/decade and a vertical thermal gradient of ca. 0.5 °C/100 m (Lampre, 2001). This value is comparable to those reported for the European Alps (up to 70 m/decade) (Brocard et al., 2013), underpinning the relationship between elevation-dependent warming and ARD. Based on this relationship a conceptual model is proposed (Fig. 12). The climate variation (i.e. warming) controls the periglacial limit migration upwards and, thus, the upper limit at which ARD processes are triggered and/or aggravated. However, this model does not explain why some nearby lakes and creeks have such different acidity condition. This suggests that the model must consider other controlling factors as the local geomorphology.

6.4. Geomorphological control

Availability of sulfide-bearing rocks is a pre-requisite for the development of ARD, but not the unique condition. So we propose that the geomorphological control, namely the nature, geometry, and arrangement of the periglacial deposits (rock glaciers, protalus ramparts, cones and talus slopes), and the DSGSD structure that affects the Monteixo-Norís range (Fig. 3B) partially causes the large variations in the acidity of the waters, both in the headwaters and in the lower parts of the catchment (Fig. 12). The hydrochemistry of the surface waters in the NVC headwaters show large differences over relatively limited areas, despite their analogous lithological and elevation contexts. For instance, the Baiau lakes show an acidity below 4–5 pH units compared by the Escorbes lakes, located just 800 m to the NW and 120 m below (Fig. 7B), despite there is no difference in the lithology at their

recharge zones (i.e. Cambro-Ordovician rhythmic sequence of schists and slates). An ARD model frequently invoked in mineralized catchments is that shallow subsurface flows derived from the melting of the ground ice of rocky periglacial deposits cause the acidification of high-elevation waters (e.g. Thies et al., 2007; Zaharescu et al., 2016; Santolaria et al., 2017; Ilyashuk et al., 2018). It is because their open-work structure, which may host groundwater, interstitial ground ice and even solid ice lenses, favors the water-rock interaction and it controls the groundwater and oxygen flows in areas dominated by low-permeability bedrock (Jóðar et al., 2017; Jones et al., 2019). All the acidic waters in the NVC drain from areas where extensive rocky periglacial deposits occur. This pattern is observed in areas such as the Pica Roja (Port Vell) and Baiau cirque sectors (Fig. 7). Here, acidic and metal-enriched seepages drain only from the extensive rock glaciers, talus slopes and cones located along the north aspect slopes. On the contrary, the Port Vell and Escorbes lakes, where the periglacial deposits are much scarcer, are not acidic, despite they are located nearby of the Pica Roja acidic seepages and Baiau acidic lakes. In the case of the Port Vell lake, just some talus slopes of limited extent are found in its recharge zone, which would explain their lower acidity. Rocky periglacial deposits are more powerful in the Escorbes recharging zone (Escorbes peak and Portella de Vallpeguera slopes) (Fig. 7B), but not as much as in the Pica Roja and Baiau sectors. This could justify that, despite not being so acidic, their waters show significant concentration in trace metals such as nickel.

That model that relates rocky detrital deposits with ARD fits well for the headwaters of the NVC, but it does not explain why acidic groundwater is also discharging via seepages and springs at the foot of the Monteixo-Norís range, at lower elevations (1860–1220 m a.s.l.), where rocky periglacial landforms are no longer found. It should be noted that the Monteixo-Norís range is affected by a sackung-type DSGSD structure (McCalpin and Irvine, 1995; Cruden and Varnes, 1996; Soldati, 2004; Pánek and Klimes, 2016), related to the Mérens shear zone (Fig. 3). Sackungs are slow-moving complexes that displace several hm³ and reach several hundred meters in depth (Soldati, 2013; Gutiérrez et al., 2012; Pánek and Klimes, 2016). These large-scale gravitational deformations cause the fracturing of rock massifs and deep circulation of fluids (e.g. Gutiérrez et al., 2005, 2008). We propose that the Monteixo-Norís sackung favors ARD processes (Fig. 12) due to the following factors: (1) it forms enclosed depressions and uphill-facing scarps that contributes to enhance surface water infiltration; (2) it creates fractures that experience significant dilation due to gravitational spreading (horizontal separation) increasing the permeability of the rock massif and the bedrock-groundwater interaction surface; (3) facilitates deeper and more rapid circulation of water and oxygen-rich air. The main groundwater discharge points in this sector are at the frontal part of the sackung, at the Noguera de Vallferrera valley, which shows a clear northward deflection attributable to the progressive displacement of the DSGSD. In such hydro-geomorphological context, several moderately acidic (pH ~4.8–6) seepages and springs discharge at elevations of 1600 to 1700 m a.s.l. (pH ~4.8–5.6); and at 1220 m a.s.l. (Areu village spring). Noticeable is the low temperature (3.9 °C) of the Mossen Batlle spring (Pla de Boet) (Fig. 3), located at a slightly higher elevation (1860 m a.s.l.). The temperature was recorded during a water sampling conducted in August 2018, while the other groundwaters were above 11 °C (Table S1 in supplementary material). This supports that the spring is not related to a shallow local flow but to a deeper and probably fast-moving groundwater flow with an elevated recharge zone (probably above 2400–2500 m a.s.l.). The Mossen Batlle spring (pH ~4.8) exhibits high concentration of metals (e.g. 1280 µg L⁻¹-Al), in the same order of magnitude as Baiau Lakes (2482 m a.s.l.) (1830–2140 µg L⁻¹-Al, with an outlier of 4890 µg L⁻¹-Al). Metal concentrations in the western sackung seepages are lower (e.g. 80–100 µg L⁻¹-Al). This apparent disagreement could be due to different reasons: (a) Samplings were conducted in different seasons, summer 2018 for Mossen Batlle and spring 2019 for the western seepages, coinciding with a snow melt peak;

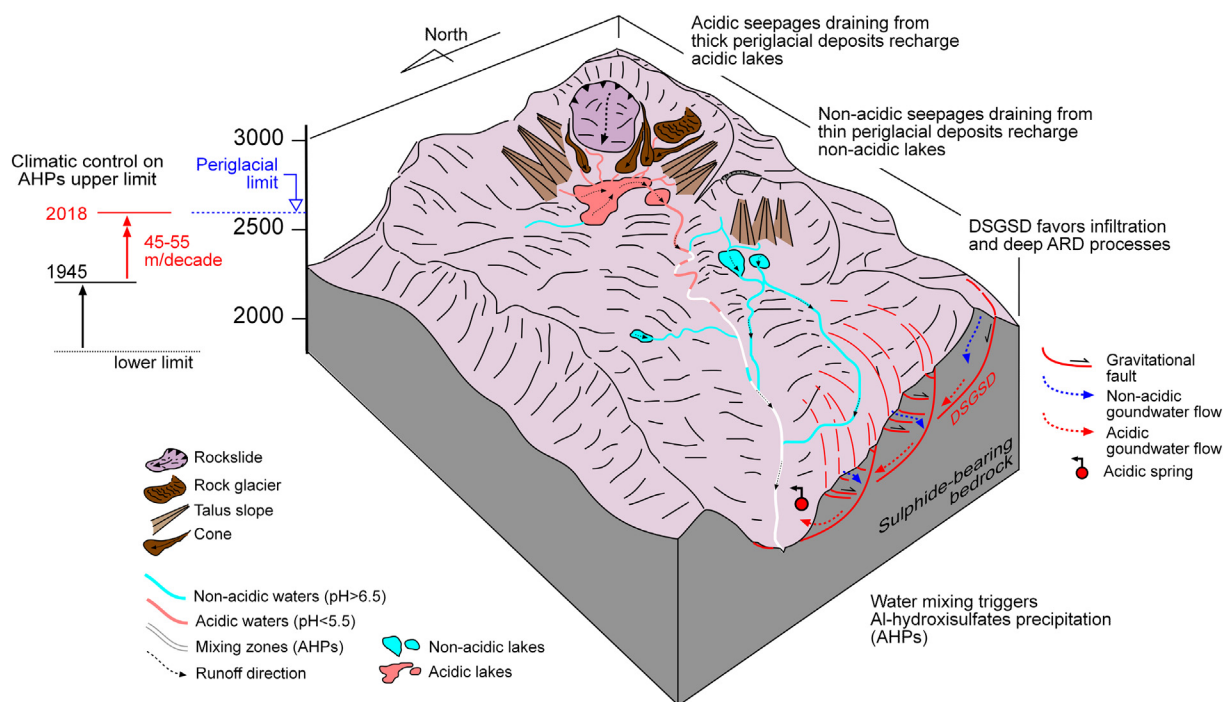


Fig. 12. Conceptual model for the different natural acid rock drainage (ARD) and Aluminum precipitation compounds (AHP) observed in the Noguera de Vallferrera catchment (NVC) controlled by climatic and geomorphological factors. Periglacial deposits and rockslides favor the development of ARD from shallow groundwater flows, while deep-seated gravitational slope deformations (DSGSDs) facilitate deeper water-rock interaction. AHPs form where acidic waters mixed with non-acidic ones. Climate warming and droughts enhance the phenomenon and the elevation at which it initiates, which has climbed hundreds of meters in recent times. The rising rates are comparable with the estimated ascending rates of the periglacial limits in the region, underpinning the proposed relationship between the effects of elevation-dependent warming and ARD intensification.

(b) Pyrite-rich slates and phyllites of the Lladorre unit crops out at elevations above 2500 m a.s.l. in the northern flank of the Monteixo-Norís Range (Fig. 1). This suggests that the metal-rich Mossen Batlle waters are recharged above this elevation, while western seepages are not. (c) The residence time of the groundwater may affect its mineral enrichment. Mossen Batlle spring is located at the NE edge of the structure, while the western seepages are in the frontal part of the sackung. Here, gravitational faulting is denser and flow paths are likely to be shorter. Unfortunately, we have no data on groundwater ages to support this hypothesis.

Climatic projections foresee a temperature increase of ca. 10 to 25% with respect to the present values in the Pyrenean region for the next 3 decades (Barrera-Escoda et al., 2014; Gonçalves et al., 2014), and similar trends are predicted for other mountain regions worldwide (Pepin et al., 2015). This future scenario leads to hypothesize that ARD processes could affect larger areas in many alpine catchments with suitable forming rocks. Therefore, a better understanding of the factors that control ARD can be valuable at designing optimal adaptation strategies for these vulnerable spaces. Furthermore, monitoring the evolution of ARD may provide useful data on climate change impacts, complementary to effects such as deglaciation and permafrost thawing. However, a comprehensive knowledge on the local geomorphological and hydrogeological context is essential for a correct interpretation of ARD patterns and to avoid potential simplifications and misleading diagnoses. In this regard, the proposed conceptual model, which considers both climatic and geomorphological factors controlling the ARD processes in the NVC, would be easily exportable to many other alpine catchments worldwide (Fig. 12).

7. Conclusions

The historical series of aerial photographs spanning more than 70 years (1945–2018) reveals that natural acid rock drainage (ARD) has experienced an intensification in the Noguera de Vallferrera Catchment

(NVC) during the last decade. ARD produces the precipitation of whitish aluminum-compounds that strikingly cover some gullies and streams in the catchment headwaters. The total length of affected streams has increased from ca. 5 km (1945–46) to more than 35 km (2018) and the maximum elevation at which ARDs initiate has climbed above 2500 m a.s.l., at rates of 45–55 m/decade. Precipitation of aluminum-compounds occurs where acidic (metal-enriched) waters are neutralized by mixing with non-acidic ones. The concentration of dissolved aluminum clearly correlates with acidity of waters, regardless of location or season. However, further research is needed to determine the patterns of seasonal variation of such concentration. In addition to aluminum, waters also exhibit anomalous concentrations of other potentially toxic trace metals such as cadmium, cobalt, copper, nickel or zinc, which largely exceed quality standards for aquatic ecosystems, and drinking water. The potential adverse effects on these pristine and vulnerable alpine ecosystems and the public health are largely unknown.

The data obtained point at there is strong climatic and geomorphological control on the ARD processes. Climate warming, markedly sharp since 1980s, in combination with the severe droughts recorded in the last decade is the most plausible cause for the ARD intensification in the study area. The rise in the maximum elevation of the ARD (45–55 m/decade) is consistent with the retreat and ascent rate of the periglacial limit in the region, estimated at 46 m/decade. The consequent degradation of permafrost facilitates that ARD intensifies at higher elevations. Geomorphological analysis reveals that pyrite-rich periglacial rocky deposits are the main ARD sources. Their high permeability and specific surface facilitate water and oxygen circulation and the biochemical oxidation of sulfides. Acidic groundwater and throughflows derived from such periglacial deposits cause the acidification of the creeks and lakes located above 2400–2500 m a.s.l. Conversely, in areas where these deposits are scarce, the phenomenon is less severe or does not manifest. Acidic seepages and springs are also at lower elevations (ca. 1860 to 1220 m a.s.l.). In these cases, acidic flows occur

associated with a deep-seated gravitational slope deformation (DSGSD) that affects the Monteixo-Norís range. Here, gravitational faulting and dilation of fractures enables the circulation of deeper oxidizing groundwater flows, permitting ARD to occur in the lower parts of the catchment. On the basis of these results, a conceptual model integrating the different ARD hydrodynamics observed in the NVC is proposed. The model proposes that, while climate warming and droughts control the intensity of ARD and its upper limits, the local hydro-geomorphology governs the spatial distribution of the affected areas.

Climatic projections foresee a sustained increase in temperature for the coming decades, which could lead to the deterioration of water resources in many cold mountain regions worldwide. Better understanding and monitoring of the evolution of natural ARD processes would be useful for predicting impacts related to climate warming and designing adaptation strategies. Understanding the geomorphological contexts of these alpine catchments, a factor which is frequently neglected, is an essential task to achieve sound diagnoses.

CRedit authorship contribution statement

Mario Zarroca: Conceptualization, Methodology, Investigation, Writing – review & editing. **Carles Roqué:** Conceptualization, Methodology, Investigation, Writing – review & editing. **Rogelio Linares:** Conceptualization, Methodology, Investigation, Writing – review & editing. **José Salminci:** Conceptualization, Methodology, Investigation, Writing – Review & Editing. **Francisco Gutiérrez:** Conceptualization, Methodology, Investigation, Writing – review & editing.

Declaration of competing interest

The authors declare that they have no known competing financial interests or personal relationships that could have appeared to influence the work reported in this paper.

Acknowledgment

This work was funded by the Fundación Biodiversidad, Ministerio para la Transición Ecológica (Gobierno de España) (grant Climate Change – 2017, PRCV00604). The work carried out by FG has been supported by project CGL2017-85045-P of the Ministerio de Ciencia e Innovación (Gobierno de España). M.Z. has a Serra Hünter fellowship at the Autonomous University of Barcelona. We thank the support of Marc Garriga, Director of the Parc Natural de l'Alt Pirineu, Eric Peramos and Blai Rosés for their technical assistance during the field work, and the anonymous reviewers and editor for their insightful comments and suggestions, which greatly improved the manuscript.

Appendix A. Supplementary data

Supplementary data to this article can be found online at <https://doi.org/10.1016/j.scitotenv.2021.146070>.

References

- Ahonen, L., Tuovinen, O.H., 1991. Temperature effects on bacterial leaching of sulfide minerals in shake flask experiments. *Appl. Environ. Microbiol.* 57, 138–145.
- Akcal, A., Koldas, S., 2006. Acid mine drainage (AMD): causes, treatment and case studies. *J. Clean. Prod.* 14, 1139–1145.
- Bacardit, M., Camarero, L., 2009. Fluxes of Al, Fe, Ti, Mn, Pb, Cd, Zn, Ni, Cu, and As in monthly bulk deposition over the Pyrenees (SW Europe): The influence of meteorology on the atmospheric component of trace element cycles and its implications for high mountain lakes. *J. Geophys. Res.-Atmos.* 114, G00D02.
- BAIC, 2019. Butlletí anual d'Indicadors Climàtics 1950–2018. Meteorological Service of Catalunya 85 pp. URL: https://static-m.meteo.cat/wordpressweb/wp-content/uploads/2018/05/29153739/BAIC2017_Resum_executiu.pdf (late access November 2019).
- Baker, B.J., Bandfield, J.F., 2003. Microbial communities in acid mine drainage. *FEMS Microbiol. Ecol.* 44, 139–152.
- Barnolas, A., Pujalte, V., 2004. La Cordillera Pirenaica. In: Vera, J.A. (Ed.), *Definición, límites y división. Geología de España. Sociedad Geológica de España – IGME, Madrid*, pp. 233–241.
- Barrera-Escoda, A., Gonçalves, M., Guerreiro, D., Cunillera, J., Baldasano, J.M., 2014. Projections of temperature and precipitation extremes in the North Western Mediterranean Basin by dynamical downscaling of climate scenarios at high resolution (1971–2050). *Climate Change* 122, 567–582.
- Bigham, J.M., Nordstrom, D.K., 2000. Iron and aluminum hydroxysulfates from acid sulfate waters. *Rev. Mineral. Geochem.* 40, 351–403.
- Blowes, D.W., Ptacek, C.J., Jambor, J.L., Weisener, C.G., 2004. The geochemistry of acid mine drainage. The geochemistry of acid mine drainage. In: Lollar, B.S., Holland, H.D., Turkian, K.K. (Eds.), *Environmental Geochemistry. Treatise on Geochemistry*. vol. 9. Elsevier-Pergamon, Oxford, UK, pp. 149–204.
- Bradley, M.W., Worland, S.C., 2015. Bibliography for acid-rock drainage and selected acid-mine drainage issues related to acid-rock drainage from transportation Activities. Open-File Report 2015–1016. U.S. Department of the Interior & U.S. Geological Survey, Reston, Virginia <https://doi.org/10.3133/ofr20151016> (24 pp.).
- Brocard, E., Philippon, R., Jeannet, P., Begert, M., Romanens, G., Levrat, G., Scherrer, S.C., 2013. Upper air temperature trends above Switzerland 1959–2011. *J. Geophys. Res. Atmos.* 118, 4303–4317.
- Camarero, L., Botev, I., Muri, G., Psenner, R., Rose, N., Stuchlik, E., 2009a. Trace elements in alpine and arctic lake sediments as a record of diffuse atmospheric contamination across Europe. *Freshw. Biol.* 54 (2518–253).
- Camarero, L., García-Pausas, J., Hugué, C., 2009b. A method for upscaling soil parameters for use in a dynamic modelling assessment of water quality in the Pyrenees. *Sci. Total Environ.* 407, 1701–1714.
- Camarero, L., Bacardit, M., de Diego, A., Arana, G., 2017. Decadal trends in atmospheric deposition in a high elevation station: effects of climate and pollution on the long-range flux of metals and trace elements over SW Europe. *Atmos. Environ.* 167, 542–552.
- Capellà, I., Carreras, J., 1996. La zonación estructural del hercínico del Pirineo central en el anticlinorio de la Pallaresa. *Estud. Geol.* 52, 51–56.
- Catalan, J., Ballesteros, E., Gacia, E., Palau, A., Camarero, L., 1993. Chemical composition of disturbed and undisturbed high-mountain lakes in the Pyrenees: a reference for acidified sites. *Water Res.* 27, 133–141.
- Choukroune, P., ECORS Team, 1989. The ECORS Pyrenean deep seismic profile reflection data and the overall structure of an orogenic belt. *Tectonics* 8, 23–39.
- Choukroune, P., Séguret, M., 1973. Tectonics of the Pyrenees, role of the gravity and compression. In: de Jong, K.H., Scholten, R. (Eds.), *Gravity and Tectonics*. Wiley, Nueva York, pp. 141–256.
- Cochelin, B., Lemirre, B., Denèle, Y., de Saint Blanquat, M., Lahfid, A., Duchêne, S.M., 2018. Structural inheritance in the Central Pyrenees: the Variscan to alpine tectonometamorphic evolution of the axial zone. *J. Geol. Soc. Lond.* 175, 336–351.
- Corella, J.P., Valero-Garcés, B.L., Wang, F., Martínez-Cortizas, A., Cuevas, C.A., Saiz-Lopez, A., 2017. 700 years reconstruction of mercury and lead atmospheric deposition in the Pyrenees (NE Spain). *Atmos. Environ.* 155, 97–107.
- Corella, J.P., Saiz-Lopez, A., Sierra, M.J., Mata, M.P., Millán, R., Morellón, M., Cuevas, C.A., Moreno, A., Valero-Garcés, B.L., 2018. Trace metal enrichment during the industrial period recorded across an altitudinal transect in the southern Central Pyrenees. *Sci. Total Environ.* 645, 761–772.
- Crouch, C.M., McKnight, D.M., Todd, A.S., 2013. Quantifying sources of increasing zinc from acid rock drainage in an alpine catchment under a changing hydrologic regime. *Hydrol. Process.* 27, 721–733.
- Cruden, D.M., Varnes, D.J., 1996. Landslide types and processes. In: Turner, A.K., Schuster, R.L. (Eds.), *Landslides: investigation and mitigation: Transportation Research Board, U.S. National Academy of Sciences, Special Report*. 247, pp. 36–75.
- Cruz-Hernández, P., Carrero, S., Sarmiento, A.M., Pérez-López, R., Cánovas, R.C., Nieto, J.M., 2012. ¿Por qué mis ríos son rojos? Hidroquímica de un ecosistema único. *Comunicaciones del XVII Simposio sobre Enseñanza de la Geología, Huelva*, pp. 344–348.
- Du, X., Wang, Y., Su, S., Li, J., 2009. Influences of pH value on the microstructure and phase transformation of aluminum hydroxide. *Powder Technol.* 192, 40–46.
- French, H.M., 2011. Periglacial. In: Singh, V.P., Singh, P. (Eds.), *Haritashya (Encyclopedia of snow, ice and glaciers)*. Springer Dordrecht, the Netherlands, pp. 827–841.
- French, H.M., 2018. *The Periglacial Environment*. 4th ed. John Wiley & Sons, Chichester, UK 544 pp.
- Furniss, G., Hinman, N.W., Doyle, G.A., Runnells, D.D., 1999. Radiocarbon-dated ferricrete provides a record of natural acid rock drainage and paleoclimatic changes. *Environ. Geol.* 37, 102–106.
- Galván, L., Olías, M., Cerón, J.C., Fernández de Villarán, R., 2021. Inputs and fate of contaminants in a reservoir with circumneutral water affected by acid mine drainage. *Sci. Total Environ.* 762, 143614.
- García-Sansegundo, J., 1996. Hercynian structure of the axial zones of the Pyrenees: the Aran Valley cross-section (Spain-France). *J. Struct. Geol.* 18, 1315–1325.
- Gault, K.B.F., Gammon, P., Fortin, D., 2015. A geochemical characterization of cold-water natural acid rock drainage at the Zn–Pb XY deposit, Yukon, Canada. *Appl. Geochem.* 62, 35–47.
- GBC (Government of British Columbia Ministry of Environment & Climate Change Strategy British Columbia), 2018. British Columbia Approved Water Quality Guidelines for Aquatic Life. Summary Report, Victoria, Canada, Wildlife & Agriculture (36pp).
- Giddings, L.A., Chlipala, G., Kunstman, K., Green, S., Morillo, K., Bhavé, K., 2020. Characterization of an acid rock drainage microbiome and transcriptome at the Ely Copper Mine Superfund site. *PLoS One* 15 (8), e0237599.
- Godt, J., Scheidig, F., Grosse-Siestrup, C., Esche, V., Brandenburg, P., Reich, A., Groneberg, D.A., 2006. The toxicity of cadmium and resulting hazards for human health. *J. Occup. Med. Toxicol.* 1, 22.

- Gonçalves, M., Barrera-Escoda, A., Guerreiro, D., Baldasano, J.M., Cunillera, J., 2014. Seasonal to yearly assessment of temperature and precipitation trends in the North-Western Mediterranean Basin by dynamical downscaling of climate scenarios at high resolution (1971–2050). *Climate Change* 122, 243–256.
- Guerrero, J., Gutiérrez, F., Carbonel, D., Bonachea, J., García-Ruiz, J.M., Galve, J.P., Lucha, P., 2013. 1:5000 landslides map of the upper Gállego Valley (central Spanish Pyrenees). *Journal of Maps* 8, 484–491.
- Gutiérrez, F., Acosta, E., Rios, S., Guerrero, J., Lucha, P., 2005. Geomorphology and geochronology of sacking features (uphillfacing scarps) in the central Spanish Pyrenees. *Geomorphology* 69, 298–314.
- Gutiérrez, F., Ortuño, M., Lucha, P., Guerrero, J., Acosta, E., Coratza, P., Piacentini, D., Soldati, M., 2008. Late quaternary episodic displacement on a sacking scarp in the central Spanish Pyrenees. Secondary paleoseismic evidence? *Geodin. Acta* 21, 187–202.
- Gutiérrez, F., Linares, R., Roqué, C., Zarroca, M., Rosell, J., Galve, J.P., Carbonel, D., 2012. Investigating gravitational grabens related to lateral spreading and evaporite dissolution subsidence by means of detailed mapping, trenching, and electrical resistivity tomography (Spanish Pyrenees). *Lithosphere* 4, 331–353.
- EEA (European Environment Agency), 2009. Regional Climate Change and Adaptation: the Alps Facing the Challenge of Changing Water Resources. Report 8, 143 pp. URL: <https://www.eea.europa.eu/publications/alps-climate-change-and-adaptation-2009> (late access November 2019).
- Huss, M., Hock, R., 2018. Global-scale hydrological response to future glacier mass loss. *Nat. Clim. Chang.* 8, 135–140.
- ICGC (Institut Cartogràfic i Geològic de Catalunya), 2007. Mapa geològic comarcal de Catalunya 1:50.000, Pallars Sobirà.
- IGC (Institut Geològic de Catalunya), 2012. Les pàtines blanques de la capçalera de la Noguera de Vallferrera. Composicions, processos i efectes associats. GAO-003/12 (89 p. Unpublished report). http://parcsnaturals.gencat.cat/web/content/home/alt_pirineu/coneix-nos/documentacio/fons_documental/biblioteca_digital/hidrologia/les_patines_blanques_a_la_cap_alera_de_la_noguera_de_vallferrera/3les_patines_blanques_de_la_cap_alera_de_la_noguera_de_vallferrera.pdf (Late access 01/26/2021).
- Ilyashuk, B.P., Ilyashuk, E.A., Psenner, R., Tessadri, R., Koinig, K.A., 2014. Rock glaciers outflows may adversely affect lakes: lessons from the past and present of two neighboring water bodies in a crystalline rock watershed. *Environ. Sci. Technol.* 48, 6192–6200.
- Ilyashuk, B.P., Ilyashuk, E.A., Psenner, R., Tessadri, R., Koinig, K.A., 2018. Rock glaciers in crystalline catchments: hidden permafrost-related threats to alpine headwater lakes. *Glob. Chang. Biol.* 24, 1548–1562.
- Jarman, D., Calvet, M., Corominas, J., Delmas, M., Gunnell, Y., 2014. Large-scale rock slope failures in the eastern Pyrenees: identifying a sparse but significant population in paraglacial and parafluvial contexts. *Geografiska Annaler, Series A, Physical Geography* 96, 357–391.
- Jarvis, I., Jarvis, K.E., 1992. Inductively coupled plasma-atomic emission spectrometry in exploration geochemistry. *J. Geochem. Explor.* 44, 139–200.
- Jean-Christophe Auguet, J.C., Casamayor, E.O., 2013. Partitioning of Thaumarchaeota populations along environmental gradients in high mountain lakes. *FEMS Microbiol. Ecol.* 84, 154–164.
- Jennings, S.R., Neuman, D.R., Blicher, P.S., 2008. Acid Mine Drainage and Effects on Fish Health and Ecology: a Review. Reclamation Research Group Publication, Bozeman, MT (26 pp).
- Jodar, J., Cabrera, J.A., Martos-Rosillo, S., Ruiz-Constán, A., González-Ramón, A., Lambán, L.J., Herrera, C., Custodio, E., 2017. Groundwater discharge in high-mountain watersheds: a valuable resource for downstream semi-arid zones. The case of the Bérchules River in Sierra Nevada (southern Spain). *Sci. Total Environ.* 593–594, 760–772.
- Jones, D.B., Harrison, E., Anderson, K., Whalley, W.B., 2019. Rock glaciers and mountain hydrology: a review. *Earth Sci. Rev.* 193, 66–90.
- Kwong, Y.T.J., Whitley, G., Roach, P., 2009. Natural acid rock drainage associated with black shale in the Yukon territory. *Canada. Appl. Geochem.* 24, 221–231.
- Lacelle, D., Doucet, A., Clark, I.D., Lauriol, B., 2007. Acid drainage generation and seasonal recycling in disturbed permafrost near Eagle Plains, northern Yukon Territory, Canada. *Chem. Geol.* 243, 157–177.
- Lampre, F., 2001. Clima de alta montaña y sistemas morfoclimáticos fríos en el macizo de la Maladeta (Pirineo aragonés). *Treballs de la Societat Catalana de Geografia* 52, 195–231.
- Laumonier, B., Abad, A., Alonso, J.L., Baudelot, S., Bresiére, G., Besson, M., Bouquet, C., Bourrouilh, R., Brula, P., Carreras, J., Centéne, A., Courjault-Rade, P., Courtessole, D., Fauconnier, D., García-Sansegundo, J., Guitard, G., Moreno-Eiris, E., Perejón, A., Vizcaino, D., 1996. Cambro-Ordovician. Synthèse géologique et géophysique des Pyrénées. 1. Édition Bureau de Recherches Géologiques et Minières (France)-Instituto Tecnológico y Geominero de España (BRGM-ITGE), pp. 157–209.
- Longerich, H.P., Jenner, G.A., Fryer, B.J., Jackson, S.E., 1990. Inductively coupled plasma-mass spectrometric analysis of geological samples: a critical evaluation based on case studies. *Chem. Geol.* 83, 105–118.
- Manning, A.H., Verplanck, P.L., Caine, J.S., Todd, A.S., 2013. Links between climate change, water-table depth, and water chemistry in a mineralized mountain watershed. *Appl. Geochem.* 37, 64–78.
- McCalpin, J., Corominas, J., 2019. Postglacial deformation history of sackungen on the northern slope of Pic d'Encampadana, Andorra. *Geomorphology* 337, 134–150.
- McCalpin, J.P., Irvine, J.R., 1995. Sackungen at the Aspen Highlands ski area, Pitkin County, Colorado. *Environ. Eng. Geosci.* 1 (3), 277–290.
- McKee, T.B., Doesken, N.J., Kleist, K., 1993. The relationship of drought frequency and duration of time scales. Eighth Conference on Applied Climatology. American Meteorological Society, Jan17–23, 1993, Anaheim, CA, pp. 179–186.
- Mertz, W., 1981. The essential trace elements. *Science* 213 (4514), 1332–1338.
- Muñoz, J.A., 1992. Evolution of a continental collision belt: ECORS-Pyrenees crustal balanced cross-section. In: McClay, K.R. (Ed.), *Thrust Tectonics*. Chapman and Hall, London, pp. 235–246.
- Nielsen, F.H., 1990. New essential trace elements for the live sciences. *Biol. Trace Elem. Res.* 26–27, 599–611.
- Nordstrom, D.K., 2009. Acid rock drainage and climate change. *J. Geochem. Explor.* 100, 97–104.
- Nordstrom, D.K., 2011a. Hydrogeochemical processes governing the origin, transport and fate of major and trace elements from mine wastes and mineralized rock to surface waters. *Appl. Geochem.* 26, 1777–1791.
- Nordstrom, D.K., 2011b. Mine waters: acidic to Circumneutral. *Elements* 7, 393–398.
- Nordstrom, D.K., Alpers, C.N., 1999. Geochemistry of acid mine waters. In: Plumlee, G.S., Logsdon, M.J. (Eds.), *The Environmental Geochemistry of Mineral Deposits*. Vol. 6A (G.S.). Soc. Econ. Geol., Littleton, Colorado, pp. 133–160 Economic Geology.
- Nordstrom, D.K., Southam, G., 1997. Geomicrobiology of sulfide mineral oxidation. In: Banfield, J.F., Nealson, K.H. (Eds.), *Geomicrobiology: Interactions Between Microbes and Minerals*. Mineralogical Society of America, Washington D.C., pp. 361–390.
- Oliva, M., Serrano, E., Gómez-Ortiz, A., González-Amuchastegui, M.J., Nieuwendam, A., Palacios, D., Pellitero-Ondicol, R., Pérez-Alberti, A., Ruiz-Fernández, J., Válcárcel, M., Vieira, G., 2016. The periglacialization of the Iberian Peninsula. *Quat. Sci. Rev.* 137, 176–199.
- Olmedo, P., Pla, A., Hernández, A.F., Barbier, F., Ayouni, L., Gil, F., 2013. Determination of toxic elements (mercury, cadmium, lead, tin and arsenic) in fish and shellfish samples. Risk assessment for the consumers. *Environ. Int.* 59, 63–72.
- OPCC-CTP, 2018. (The Pyrenees Climate Change Observatory), 2019. El cambio climático en los Pirineos: impactos, vulnerabilidades y adaptación. Bases de conocimiento para la futura estrategia de adaptación al cambio climático en los Pirineos, Madrid, Spain 150 pp. <https://www.opcc-ctp.org/sites/default/files/documentacion/opcc-inform-es-print.pdf> (late access April 2020).
- Pánek, T., Klimes, J., 2016. Temporal behavior of deep-seated gravitational slope deformations: a review. *Earth Sci. Rev.* 156, 14–38.
- Pepin, N., Bradley, R.S., Díaz, H.F., Baraer, M., Caceres, E.B., Forsythe, N., Fowler, H., Greenwood, G., Hashmi, M.Z., Liu, X.D., Miller, J.R., Ning, L., Ohmura, A., Palazzi, E., Rangwala, I., Schöner, W., Severskiy, I., Shahgedanova, M., Wang, M.B., Williamson, S.N., Yang, D.Q., 2015. Elevation-dependent warming in mountain regions of the world. *Nat. Clim. Chang.* 5, 424–430.
- Pérez-Zanón, N., Sigró, J., Ashcroft, L., 2017. Temperature and precipitation regional climate series over the Central Pyrenees during 1910–2013. *Int. J. Climatol.* 37, 1922–1937.
- Pla, S., 2001. Chrysophycean cysts from the Pyrenees. *Bibl. Phycol.* 109, 1–179.
- Plaza, F., Wen, Y., Perone, H., Xu, Y., Liang, X., 2017. Acid rock drainage passive remediation: potential use of alkaline clay, optimal mixing ratio and long-term impacts. *Sci. Total Environ.* 15, 572–585.
- Plumlee, G.S., Smith, K.S., Montour, M.R., Ficklin, W.H., Mosier, E.L., 1999. Geologic controls on the composition of natural waters and mine waters. In: Filipek, L.H., Plumlee, G.S. (Eds.), *The Environmental Geochemistry of Mineral Deposits. Part B: Case Studies and Research Topics*. v. 6B. Society of Economic Geologists, Reviews in Economic Geology, pp. 373–432 Chapter 1.
- Qian, G., Li, Y., 2019. Acid and metalliferous drainage—a global environmental issue. *Journal of Mining & Mechanical Engineering* 1, 1–4.
- Radić, V., Bliss, A., Beedlow, A.C., Hock, R., Miles, E., Cogley, J.G., 2014. Regional and global projections of twenty-first century glacier mass changes in response to climate scenarios from global climate models. *Clim. Dyn.* 42, 37–58.
- Rezaie, B., Anderson, A., 2020. Sustainable resolutions for environmental threat of the acid mine drainage. *Sci. Total Environ.* 717, 137211.
- Rosell, J., Linares, R., 2001. Grandes deslizamientos en el frente de la lámina cabalgante del Montsec (Sierra del Montsec, Prepirineo Central). *Rev. Soc. Geol. Esp.* 14, 255–268.
- Salerno, F., Rogora, M., Balestrini, R., Lami, A., Tartari, G.A., Thakuri, S., Tartari, G., 2016. Glacier melting increases the solute concentrations of Himalayan glacial lakes. *Environ. Sci. Technol.* 50, 9150–9160.
- Sánchez-España, J., 2007. The behavior of Iron and aluminum in acid mine drainage: speciation, mineralogy, and environmental significance. In: Letcher, T.M. (Ed.), *Thermodynamics, Solubility and Environmental Issues*. Elsevier Science, Amsterdam, The Netherlands, pp. 137–150.
- Sánchez-España, J., Yusta, I., Diez, M., 2011. Schwertmannite and hydrobasaluminite: a re-evaluation of their solubility and control on the iron and aluminum concentration in acidic pit lakes. *Appl. Geochem.* 26, 1752–1774.
- Sánchez-España, J., Yusta, I., Burgos, W.D., 2016. Geochemistry of dissolved aluminum at low pH: Hydrobasaluminite formation and interaction with trace metals, silica and microbial cells under anoxic conditions. *Chem. Geol.* 441, 124–137.
- Santolaria, Z., Arruebo, T., Pardo, A., Rodríguez-Casals, C., Matesanz, J.M., Lanaja, F.J., Urieta, J.S., 2017. Natural and anthropic effects on hydrochemistry and major and trace elements in the water mass of a Spanish Pyrenean glacial lake set. *Environ. Monit. Assess.* 189 (7), 324.
- Sarmiento, A.M., DelValls, A., Nieto, J.M., Salamaña, M.J., Caraballo, M.A., 2011. Toxicity and potential risk assessment of a river polluted by acid mine drainage in the Iberian Pyrite Belt (SW Spain). *Sci. Total Environ.* 409, 4763–4771.
- Schoonen, M., Elsetinow, A., Borda, M., Strongin, D., 2000. Effect of temperature and illumination on pyrite oxidation between pH 2 and 6. *Geochem. Trans.* 1, 1–23.
- Serrano, E., Morales, C., González Turba, J.J., Martín, R., 2009. Cartografía del permafrost de montaña en los Pirineos españoles. *Finisterra XLIV* 87, 45–54.
- Soldati, M., 2004. Deep-seated gravitational slope deformation. In: Goudie, A.S. (Ed.), *Encyclopedia of Geomorphology*. vol. I. Routledge, New York, pp. 226–228.

- Soldati, M., 2013. Deep-seated gravitational slope deformation. In: Bobrowsky, P.T. (Ed.), *Encyclopedia of Natural Hazards*. Encyclopedia of Earth Sciences Series. Springer, Dordrecht, pp. 151–155.
- Takeno, N., 2005. Atlas of Eh-pH Diagrams. INTERCOMPARISON OF Thermodynamic Data-bases. National Institute of Advanced Industrial Science and Technology, Geological Survey of Japan Open File Report No. 419, Japan 285 pp.
- Talukdar, B., Kalita, H.K., Baishya, R.A., Basumatary, S., Sarma, D., 2016. Evaluation of genetic toxicity caused by acid mine drainage of coal mines on fish fauna of Simsang River, Garohills, Meghalaya, India. *Ecotoxicol. Environ. Saf.* 131, 65–71.
- Teixell, A., Muñoz, J.A., 2000. Evolución tectono-sedimentaria del Pirineo meridional durante el Terciario: Una síntesis basada en la transversal del Río Noguera-Ribagorçana. *Rev. Soc. Geol. Esp.* 13, 251–264.
- Thies, H., Nickus, U., Mair, V., Tessadri, R., Tait, D., Thaler, B., Psenner, R., 2007. Unexpected response of high alpine lake waters to climate warming. *Environ. Sci. Technol.* 41, 7424–7429.
- Todd, A.S., Manning, A.H., Verplanck, P.L., Crouch, C., McKnight, D.M., Dunham, R., 2012. Climate-change-driven deterioration of water quality in a mineralized watershed. *Environ. Sci. Technol.* 46, 9324–9332.
- Tuffnell, S., 2017. Acid Drainage: the Global Environmental Crisis You've Never Heard Of. <https://theconversation.com/acid-drainage-the-global-environmental-crisis-youve-never-heard-of-83515>.
- Turú, V., Planas, X., 2005. Inestabilidad de vertientes en los valles del Valira. Datos y dataciones para el establecimiento de una cronología, posibles causas. Andorra y Alt Urgell (Pirineos orientales). VI Simposio Nacional sobre Taludes y Laderas Inestables, Valencia (Abstracts).
- Williams, M.W., Knauf, M., Caine, M., Liu, F., Verplanck, P.L., 2006. Geochemistry and source water of rock glacier outflow. Colorado Front Range. *Permafrost. Periglacial Process.* 17, 13–33.
- Zaharescu, D., Hooda, P., Burghilea, C., Polyakov, V., Palanca-Soler, A., 2016. Climate change enhances the mobilization of naturally occurring metals in high altitude environments. *Sci. Total Environ.* 560–561, 73–81.
- Zaharescu, D.G., Hooda, P.S., Fernandez, J., Palanca-Solera, A., Ionela-Burghilea, C., 2009. On the arsenic source mobilisation and its natural enrichment in the sediments of a high mountain cirque in the Pyrenees. *J. Environ. Monit.* 11, 1973–1981.
- Zandvliet, J., 1960. The geology of the upper Salat and Pallaresa Valleys, Central Pyrenees, France - Spain. *Leidsche Geol. Meded.* 33, 191–254.